An *In Situ* MBfR System to Treat Nitrate-Contaminated Surface Water

by

Yizhou Li

A Thesis Presented in Partial Fulfillment
of the Requirements for the Degree
Master of Science

Approved November 2014 by the
Graduate Supervisory Committee:

Bruce Rittmann, Chair
Enrique Vivoni
Rosa Krajmalnik-Brown

ARIZONA STATE UNIVERSITY

December 2014

ABSTRACT

Nitrate, a widespread contaminant in surface water, can cause eutrophication and toxicity to aquatic organisms. To augment the nitrate-removal capacity of constructed wetlands, I applied the H_2-based Membrane Biofilm Reactor (MBfR) in a novel configuration called the *in situ* MBfR (isMBfR). The goal of my thesis is to evaluate and model the nitrate removal performance for a bench-scale isMBfR system.

I operated the bench-scale isMBfR system in 7 different conditions to evaluate its nitrate-removal performance. When I supplied H_2 with the isMBfR (stages 1 – 6), I observed at least 70% nitrate removal, and almost all of the denitrification occurred in the "MBfR zone." When I stopped the H_2 supply in stage 7, the nitrate-removal percentage immediately dropped from 92% (stage 6) to 11% (stage 7). Denitrification raised the pH of the bulk liquid to ~ 9.0 for the first 6 stages, but the high pH did not impair the performance of the denitrifiers. Microbial community analyses indicated that DB were the dominant bacteria in the "MBfR zone," while photosynthetic Cyanobacteria were dominant in the "photo-zone".

I derived stoichiometric relationships among COD, alkalinity, H_2, Dissolved Oxygen (DO), and nitrate to model the nitrate removal capacity of the "MBfR zone." The stoichiometric relationships corresponded well to the nitrate-removal capacity for all stages expect stage 3, which was limited by the abundance of Denitrifying Bacteria (DB) so that the H_2 supply capacity could not be completely used.

Finally, I analyzed two case studies for the real-world application of the isMBfR to constructed wetlands. Based on the characteristics for the wetlands and the stoichiometric relationships, I designed a feasible operation condition (membrane area

and H_2 pressure) for each wetland. In both cases, the amount of isMBfR surface area was modest, from 0.022 to 1.2 m^2/m^3 of wetland volume.

ACKNOWLEDGMENTS

I would like to thank my advisor, Dr. Bruce Rittmann, for his invaluable guidance and great help through my entire MS program. I can't appreciate enough for his lessons on how to perform mass balance, and how to write reports and thesis. I also thank him for his excellent comments and "take-home massages" for my research and thesis. I would like to express my appreciation to my committee members Dr. Rosa Krajmalnik-Brown and Dr. Enrique Vivoni for their assistance and expertise.

I would like to thank Diane Hagner for her great help during the time I spent in Swette Center. I would like to thank Dr. Yonghong Wu, the visiting scholar from China, for teaching me a lot about the idea of *in situ* MBfR. I also gratefully acknowledge Luis Ordaz Diaz, the visiting scholar from Mexico, for doing the sampling and measurement work with me during my research.

I am deeply grateful to Dr. Aura Ontiveros, my research mentor, who trained me on the Membrane Biofilm Reactor (MBfR) and offered me so much excellent advice on my research and thesis. I also appreciate her for helping me analyze the microbial community in my reactor. I owe thanks to Alex Zevin for helping me analyze the microbial community for cyanobacteria. I owe thanks to Dr. Chen Zhou and Zhuolin Liu for helping me measure the Dissolved Oxygen concentration.

Finally, I would like to thanks my parents for supporting me to study in Arizona State University and providing me the endless love and courage.

TABLE OF CONTENTS

Page

CHAPTER Page

LIST OF TABLES

LIST OF FIGURES

Figure Page

CHAPTER 1

INTRODUCTION AND BACKGROUND

1.1 Nitrate Contamination in Surface Water

Due to the human activities, large amounts of nitrate are discharged into aquatic environments. High loadings of nitrate and other nitrogen sources may degrade aquatic ecosystems through eutrophication. Because nitrogen is a limiting nutrient in aquatic and terrestrial ecosystems (Vitousek & Howarth, 1991), high loadings of nitrate in the aquatic ecosystem will stimulate the growth of phytoplankton, resulting in harmful algae blooms, a decrease of the species diversity, and deterioration of water quality (Smith et al., 1999). The degradation of the aquatic ecosystem will reduce economic benefits from recreation, industrial use, and agriculture (Carpenter et al., 1997).

A high concentration of nitrate also can lead to toxic effects to aquatic organisms (Cheng & Chen, 2002; Jensen, 1996). In anaerobic conditions, nitrate can be converted to nitrite, which is more toxic. Although USEPA has recommended a maximum contaminant level (MCL) for nitrate of 10 mg-N/L for drinking water, no nitrate standard is in effect for protecting aquatic life (US Environmental Protection Agency, 1986). Ironically, 10 mg-N/L has adverse effects on the aquatic organisms during long-term exposure, and Camargo et al. (2005) recommended a safe nitrate level of 2.0 mg-N/L for the aquatic organism based on nitrate-toxicity data to freshwater animals.

Urban and agricultural activities are two major reasons for the high loading of nitrate in aquatic systems. Urban areas discharge nitrate to aquatic systems through storm-water runoff and municipal wastewater effluent. Large amounts of nitrate waste can be released through sewage leakage, application of fertilizer, and the atmospheric

deposition. Groffman (2004) reported 75% nitrogen retention of in an urban ecosystem, which indicates that majority of nitrogen accumulates inside the urban area. During a storm, the accumulated nitrate can migrate with rainwater and enter the aquatic system. In addition, nitrate often remains in the effluent of wastewater treatment plants unless tertiary treatment is applied to remove it (Day, 2004).

Agricultural runoff is the largest source of nitrate to surface water. To achieve a high crop production, nitrogen fertilizer is applied to croplands, but only part of the applied nitrogen is used by the crops; the remaining nitrogen fertilizer accumulates in the soil and migrates to the aquatic system in irrigation water and rainwater. Livestock farming, such as dairy farming, is another nitrogen source in agricultural runoff. However, unlike the runoff from cropland, runoff from livestock farming contains high concentration of organic matter, along with nitrogen compounds (McGechan, 2005).

1.2. Methods to Treat Nitrate in Surface Water

1.2.1 Nitrate Removal through Wastewater Treatment Plants

One method to remove nitrate from surface water is to treat the nitrate-contaminated surface water by passing it through a treatment plant. Ion exchange and biological denitrification are two widely applied nitrate-removal processes (Stevenson, 1997). Ion exchange replaces the nitrate anion with another anion, often chloride, present in an ion-exchange resin; once the resin is saturated with nitrate, it can be regenerated by using a NaCl brine. Although ion exchange is able to achieve high removal efficiency, it cannot destroy the nitrate ion, but moves it to another location, normally the regeneration brine (WHO, 2004). Another drawback of ion exchange is that the resin is easily fouled by organic matter or suspended solids.

Biological denitrification utilizes the natural activity of nitrate-respiring bacteria to reduce nitrate to nitrogen gas. When a suitable electron donor and carbon source are present in the water, denitrifying bacteria reduce nitrate to nitrogen gas when the conditions are sufficiently anoxic (Rittmann & McCarty, 2001). With sufficient electron donor, nitrate can be completely removed and converted to harmless N_2 gas. When organic matter is present in the water, it can act as electron donor and carbon source to drive the denitrification process. When no organic matter is present in the water, an exogenous donor, such as methanol or hydrogen, must be added.

Other advanced treatment methods, such as reverse osmosis, also are capable to remove nitrate from wastewater; however, due to the high cost, they are not widely used for nitrate removal in waste water treatment plants (Stevenson, 1997). Thus, ion exchange and denitrification are the main competing options.

1.2.2 Nitrate Removal through Constructed Wetlands

Wetlands have self-purification ability through physical, chemical, and biological processes (Vagnetti et al., 2003). Previous research indicates that wetlands can remove nitrate, ammonium, phosphate, heavy metals, and organic matter (Kadlec & Knight, 2008). Taking advantage of the natural self-purification ability of wetlands, artificial wetlands – also called constructed wetlands -- can be designed to treat different kinds of wastewater. By selecting suitable plants and proper design criteria -- including retention time, wetland area, and water depth -- artificial wetlands can achieve different treatment goals (Mansor et al., 2002). So far, constructed wetlands have been applied to treat domestic wastewater, animal wastewater, mine water, industrial wastewater, urban storm-water, and agricultural runoff (Kadlec & Knight, 2008).

Advantages of constructed wetlands are low cost and low energy consumption, compared with wastewater treatment plants (Day, 2004). Constructed wetlands do not need large investment for facilities, and energy needed for operation is minimal. Another advantage of a constructed wetland is that its removal efficiency is more predictable than that of a natural wetland. The nitrogen-removal kinetics for constructed wetland have been successfully described through a simple first-order model, and the first-order model could be used to estimate the needed surface area to achieve a treatment goal (Arheimer & Wittgren, 2002; Karpuzcu & Stringfellow, 2012).

Constructed wetland can remove nitrate in surface water through plant uptake and biological denitrification. When ammonia is not present in the environment, nitrate can be an alternative nitrogen source, and aquatic plants will take up nitrate in water and convert it to organic nitrogen. As a result, nitrate is removed from water. However, to remove this part of nitrogen, plant harvesting is needed; otherwise, this part of nitrogen will return to ecosystem in the form of organic nitrogen or ammonia due to the decomposition of dead plant material. Biological denitrification is another important nitrate-removal mechanism in a constructed wetland. Unlike plant uptake, biological denitrification can reduce nitrate to nitrogen gas and remove nitrogen from the aquatic ecosystem. Heterotrophic denitrification is the dominant biological denitrification process in constructed wetlands, and organic carbon is the primary electron donor and carbon source for heterotrophic denitrification process. The organic carbon comes from the organic matter in the influent, the decomposition of dead plants, and organic compounds released by plant roots (Lynch, 1990).

Constructed wetlands have been successfully applied to treat nitrate contamination in urban and livestock-farming runoff. Urban runoff includes municipal wastewater effluent and storm-water runoff, and both are characterized by a low nitrate concentration (Collins et al., 2010; Day, 2004). Beutel et al. (2009) reported that at low nitrate concentration (<3 mg-N/L), constructed wetland can achieve nitrate removal over 90%.

Runoff from livestock farming, on the other hand, is characterized by high concentration of organic carbon, as well as nitrogen compounds (including nitrate, ammonium, and organic nitrogen). Since organic carbon can favor biological denitrification, high nitrate removal is possible.

Since heterotrophic denitrification is a major nitrate-removal mechanism, the performance of constructed wetland can be limited by the concentration of electron donor, organic carbon in this case. Organic matter in the influent normally is the important electron source to support denitrification. The performance of a constructed wetland may be impaired when the surface water has a high nitrate concentration and a low Chemical Oxygen Demand (COD); cropland runoff is a common example. Poe et al. (2003) reported nitrate removal of 59% when treating cropland runoff through a constructed wetland, and only 13% of the nitrate was removed by denitrification.

In summary, constructed wetlands can be a cost-effective means to remove nitrate from surface water, but the performance of a constructed wetland often is limited by the amount of organic electron donor. Therefore, an alternative approach is needed to treat water that contains a high concentration nitrate and a low concentration of organic matter.

1.3 A Review of H_2 Based Membrane Biofilm Reactor (MBfR)

The H_2-based membrane biofilm reactor (MBfR) is a promising alternative for overcoming electron-donor limitation for denitrification. In the MBfR, H_2 gas is an inorganic electron donor that replaces the traditional organic donor. Compared with organic electron donors, H_2 has several advantages: (1) the carbon source is inorganic carbon, which is ubiquitous in the environment; (2) less biomass is formed; (3) its cost per electron delivered is lower; and (4) it has no toxicity to humans or microorganisms (Martin & Nerenberg, 2012). However, due to its low solubility, H_2 cannot be delivered efficiently by normal gas-delivery methods. As was first illustrated by Lee and Rittmann (2000), the challenge of H_2 delivery as an electron donor can be overcome with the MBfR.

In MBfR, H_2 diffuses through the walls of non-porous membranes. Autotrophic denitrifiers form a biofilm on the outside wall of the membrane and utilize H_2 from the membrane while reducing nitrate from the liquid. The H_2-delivery capacity can be easily regulated by the H_2 pressure to the membranes (Lee & Rittmann, 2002; Tang et al., 2012), and escaped H_2 usually is negligible.

Because H_2 can act as an excellent electron donor for all microorganism-based respirations, the MBfR has the ability to remove other oxidized contaminants in water: e.g., selenate, chromate, perchlorate, and TCE (Chung et al., 2008; Lee & Rittmann, 2000; Van Ginkel et al., 2011; Ziv-El & Rittmann, 2009).

The goal is that the oxidized contaminants are removed and that no excess H_2 escapes from the reactor. Thus, managing H_2 delivery is important to the performance of MBfR. Tang et al. (2012) measured the H_2 permeability of three types of hollow fibers

(composite, polyester, and polypropylene) used in the MBfR and developed unique linear relationships between H_2 pressure and H_2 delivery capacity for each fiber type. These linear relationships enable us to manage the H_2 delivery capacity and match it to the amount of H_2 needed to achieve the desired level of contaminant removal while avoiding release of excess H_2.

The H_2-based MBfR has been applied at pilot scale to remove nitrate and perchlorate from groundwater, and high removal efficiency has been achieved without causing new water-quality problems (Tang et al., 2010; Zhao et al., 2014). In addition, economic analyses show that, compared with other treatment methods, the MBfR can save on operating costs due to the low energy demand and reduced utilization of electron donor (Martin & Nerenberg, 2012). Thus, the H_2-based MBfR is a promising alternative for treating a wide range of waters contaminated with nitrate and other oxidized contaminants. Up to now, it has been used for "end of pipe" treatment of groundwater or surface water. The next section describes how the MBfR can be adapted for *in situ* removal of nitrate, such as in a constructed wetland.

1.4 *In Situ* MBfR System

1.4.1 Description of an *In Situ* MBfR System

The *in situ* MBfR (isMBfR) is a novel application of the H_2-based MBfR. Its goal is to remove nitrate from contaminated surface water, such as in a constructed wetland. The goal is to augment the natural capability of the wetland for denitrification so that nitrate removal is complete and reliable.

Figure 1 shows the concept of an isMBfR. An isMBfR module is placed in the deep layer of a constructed wetland to remove nitrate that either enters with the inflow or

is produced in the aerobic upper layers that have aquatic plants and phytoplankton (Rittmann, 2013). H_2 is delivered to the isMBfR modules from the delivery port in the top and supports autotrophic denitrification by biofilms that accumulate on the membrane walls. The isMBfR module is inspired by the MBfR module for pilot-scale treatment (Evans et al., 2013) and consists of a perforated core in the center and fiber sheets wrapped around the core (shown in Figure 2). The fiber sheets contain thousands of fibers. The fibers are connected to the H_2 delivery port in the top so that H_2 gas can be delivered into the lumen of fibers. During operation, H_2 gas diffuses from the lumen of fibers, through the fiber walls, and into the biofilm of autotrophic denitrifiers to reduce nitrate to nitrogen gas.

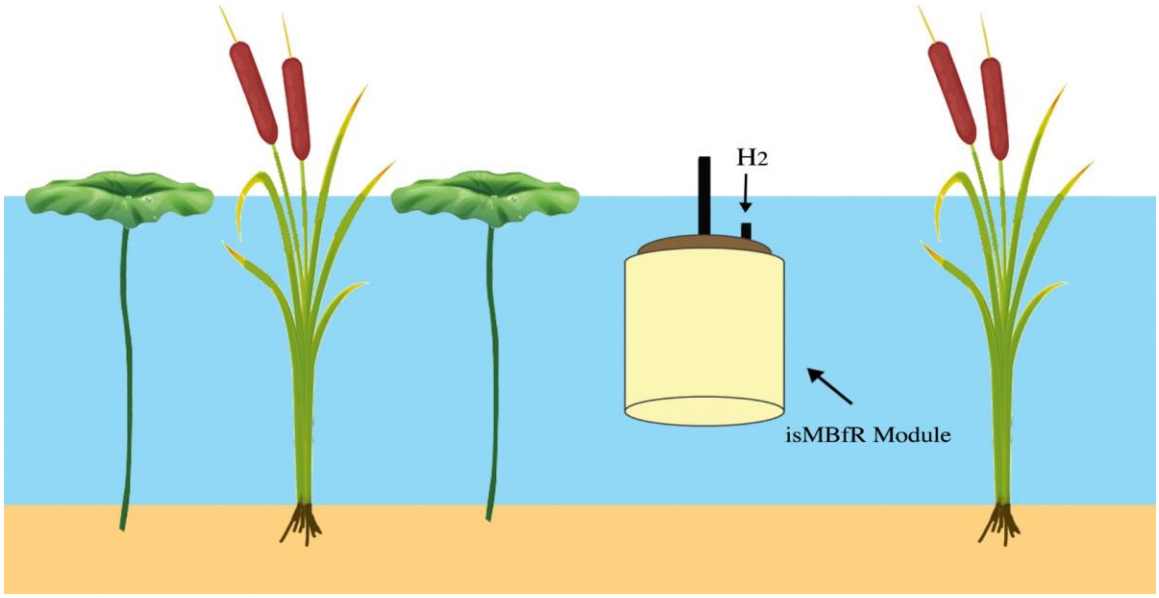

Figure 1. The concept of the isMBfR for enhancing denitrification in a constructed wetland. A pump is set in the bottom of the module to pump water into the perforated core.

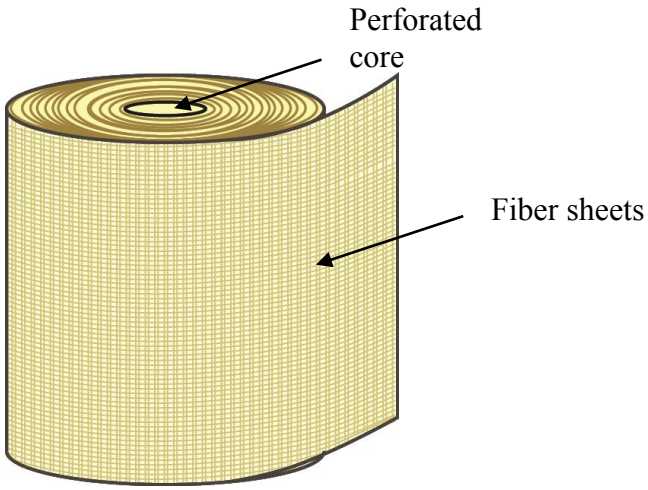

Figure 2. The structure of an isMBfR module.

The aquatic plants and phytoplankton living near the top of the wetland also may contribute to nitrate removal. Through photosynthesis, they produce biomass. Nitrogen is removed when the biomass is harvested. In addition, the biomass can become an organic electron donor to drive denitrification when it decays. Furthermore, the decay of the biomass decreases the dissolved oxygen concentration, which enhances denitrification. On the other hand, the upper zones are likely to have elevated dissolved oxygen during active photosynthesis. High enough concentration of dissolved oxygen (~ 5 mg/L) stops denitrification (de Silva & Rittmann, 2000), and the reduction of O_2 as an electron acceptor increased the demand for all donors, including H_2.

In summary, the isMBfR is a novel mean to deliver H_2 to drive denitrification in surface water. Aquatic plants and phytoplankton may enhance or impair nitrogen removal, but the main role of the isMBfR is to increase the reduction of NO_3^- to N_2 beyond what is possible with only the naturally occurring processes of denitrification and plant uptake.

1.4.2 Quantifying the Impact of an isMBfR in a Constructed Wetland

In many situations, constructed wetlands cannot meet treatment objectives (Arheimer & Wittgren, 2002). Although installation and operation of an isMBfR involves costs, it offers the possibility of greater and more reliable nitrogen removal, thus overcoming the well-known deficiencies of wetlands. This section builds a simple model to evaluate when the isMBfR can have a significant benefit for the performance of a constructed wetland.

According to Kadlec and Knight (2008), the performance of constructed wetland can be described by a first-order model:

$$J_{CN} = k_{CN} C_N \qquad Eq.(1)$$

J_{CN} is the nitrate removal flux in constructed wetland (g/m^2-d), k_{CN} is the removal rate constant for constructed wetland (m/yr), C_N is the nitrate concentration (g/m^3), and the area (m^2) for J_{CN} is the plan-view surface area of the wetland. The mass/time removal of nitrate can be calculated based on Eq. (1):

$$R_{CN} = J_{CN} A_C = k_{CN} C_N A_C \qquad Eq.(2)$$

R_{CN} is the mass/time removal rate of nitrate in constructed wetland (g/d), and A_C is the plan-view surface area of the constructed wetland (m^2).

From Eq. 1, the performance of a constructed wetland depends on the removal rate constant and the surface area. A low k_{CN} value, insufficient surface area, or both will limit the performance of constructed wetland. In principle, A_C could be increased to compensate for low J_{CN}, but sufficient land often is not available. For example, Arheimer and Wittgren (2002) reported a scenario in southern Sweden that only 0.4% of total area

can be used for constructed wetland, because landowners are unwilling to convert their lands to constructed wetland.

isMBfR modules can be added to the wetland to augment performance. The performance of isMBfR modules can be described by:

$$R_{IN} = J_{IN} A_M \qquad Eq.(3)$$

R_{IN} is the mass/time nitrate removal in the isMBfR modules (g/d), J_{IN} is the nitrate flux of isMBfR modules (g/m^2-d), and A_M is the total surface area of membranes (m^2). The performance of isMBfR modules depends on the nitrate flux and membrane surface area. The nitrate flux is related to the H_2 flux, which can be controlled by H_2 pressure. The membrane surface area is determined by the number of modules installed.

The overall mass/time nitrate removal for an isMBfR system is the sum of R_{CN} and R_{IN}:

$$R_{TN} = R_{CN} + R_{IN} = k_{CN} C_N A_C + J_{IN} A_M \quad Eq.(4)$$

R_{TN} is the total mass/time nitrate removal rate in an isMBfR system (g/d). According to Eq. (4), we can compensate the insufficient land area (A_C) by either increasing J_{IN}, A_M, or both. J_{IN} can be increased by raising H_2 pressure, while A_M can be increased by adding the number of isMBfR modules. Since higher J_{IN} and A_M are much more achievable than higher A_C, isMBfRs can easily augment the performance of constructed wetland and deal with high nitrate loading.

In addition, isMBfRs provide the ability to deal with fluctuating nitrate loading by adjusting the H_2 pressure so that the total nitrate-removal capacity matches the nitrate loading. Then, the effluent nitrate concentration can be kept low level even the nitrate loading increases.

In summary, the isMBfR system is well suited for situations in which the performance of a constructed wetland is limited by low k_{CN} value, low surface area, and high variability in nitrate loading.

1.4.3 Concerns with the isMBfR

Although the isMBfR is a promising alternative to treat nitrate-contaminated surface water, a number of concerns need to be addressed:

(1) An isMBfR will remove virtually all the dissolved oxygen in the water surrounding it. Since higher life forms require a significant dissolved-O_2 concentration, parts of the constructed wetland will become uninhabitable by fish, for example. If higher life forms are part of the ecosystem of the constructed wetland, the design must provide for sufficient habitat with high dissolved O_2.

(2) Excess delivery of H_2 should be avoided for three reasons. First, H_2 is a combustible gas when mixed at certain ratios with O_2. Off-gassing of H_2 should be avoided as a safety precaution. Second, sulfate almost always is present in surface water. Excess delivery of H_2 may cause sulfate reduction to H_2S, which is odorous and also can be toxic. Lower nitrate surface loading and high H_2 delivery capacity are known to lead to sulfate reduction. For example, Ontiveros et al. (2012) reported that sulfate is reduced when the NO_3^- + O_2 surface loading is lower than 0.15 g H_2/m^2-day, while Zhao et al. (2014) reported that sulfate reduction happened when the NO_3^- + O_2 surface loading was lower than 0.18 g H_2/m^2-d. Third, the delivery of excess H_2, no matter its fate, is an unnecessary cost.

(3) Phototrophic microorganisms, such as algae and cyanobacteria, may elevate the DO concentration level through photosynthesis. High DO concentration level can weaken denitrification by either inhibiting the denitrification rate, increase H_2 demand, or both. It may be necessary to limit the growth and activity of phototrophic microorganisms, such as by shading or harvesting.

1.5 Objective

The objective of this thesis is to evaluate and model the performance of a bench-scale model of the isMBfR system in a constructed wetland. I applied a bench-scale isMBfR to treat nitrate-contaminated water in 7 different conditions. I used the nitrate-removal rates and percentages for each of the 7 conditions as the primary indicators of performance of the isMBfR. In addition, I used stoichiometry to derive mathematical relationships among nitrate, O_2, H_2, COD, and alkalinity. Then, I modeled the nitrate-removal capacity of the isMBfR through the relationships and assessed the model results through the comparison between the estimated results and experimental results. Finally, I took bacterial samples in 3 stages and had the microbial community analyzed to help explain the performance of isMBfR.

My thesis consists of the 5 following chapters, whose objectives I summarize here.

1. In chapter 2, I describe the setup of the bench-scale wetland, particularly the locations of the isMBfR fibers and the sample ports. I summarize the conditions in 7 stages and the methods to analyze the liquid samples taken from each stage. Finally, I describe the methods to take and analyze the biofilm sample.

2. In chapter 3, I summarize the results in each stage, including the concentrations of nitrate, nitrite, sulfate, COD, and alkalinity, along with the pH. I calculate the mass/time nitrate and COD removals contributed by "MBfR zone," "photo-zone," and effluent tubing separately. Then, I calculate the removal percentage of nitrate for each stage and gauge the performance in each stage.
3. In chapter 4, I derive the mathematical relationships among nitrate, H_2, COD, and alkalinity, and I model the nitrate removal capacity for the bench-scale isMBfR based on the relationships. I evaluate the model results by comparing it with the experimental results.
4. In chapter 5, I summarize the results for the microbial community analysis for stages 2, 3, and 6. The abundances of general bacteria, denitrifying bacteria, and sulfate-reducing bacteria were measured through Quantitative Polymerase Chain Reaction (qPCR) for the "MBfR zone" and the "photo-zone," and photosynthetic microorganisms were observed through light microscopy for the "photo-zone." I use the microbial community data to help explain the performance of isMBfR and the model results evaluated in the previous chapters.
5. In chapter 6, I summarize the results and apply the isMBfR system to real wetlands where the nitrate removal capacities are lower than the nitrate loadings. I also make some suggestions for future research for the isMBfR system.

CHAPTER 2

MATERIALS AND METHODS

2.1 Experimental Setup

As shown in Figure 3, the isMBfR reactor consisted of 2 compartments, the "MBfR zone" in the bottom and the "photo-zone" in the top. The "photo-zone" simulated the activity of macrophytes and phytoplankton in the surface of a wetland. In this compartment, 150 cm^3 of low-density (18 kg/m^3) sponges was employed to support the growth of phytoplankton (such as photosynthetic bacteria). During the experimental period, phytoplankton living in this compartment produced O_2 and biomass through photosynthesis. The bottom part was where the H_2-based MBfR was located to augment nitrate removal through autotrophic denitrification. This compartment held 7 bundles (with a total surface area of 0.07 m^2) of polypropylene fibers (products of Teijin Fibers Ltd., Osaka, Japan) sealed into H_2 ports to deliver H_2. The other ends of the fibers were shut with glue. Each bundle consisted of 12 fibers of 13-cm length. During experimentation, H_2 was supplied from the top through tubing and distributed to the 7 H_2 ports. Autotrophic denitrifiers accumulated on the fiber walls and utilized H_2 to reduce nitrate, as well as O_2 to produce H_2O. The top and bottom compartments were separated by a floating support, the device used to deliver H_2 to the MBfR fibers. The volume of the top compartment (above the floating support) was ~ 210 mL (with a liquid volume of about 150 mL), and the volume of the bottom compartment (below the floating support and holding the isMBfR) was ~450 mL.

Figure 3 shows the experimental setup when COD was not supplied to the reactor. The synthetic water was contained in one tank and fed to the reactor through a pump

throughout the experiments. The synthetic water entered at the bottom. A stir bar at the bottom of the "MBfR zone" kept the liquid in the "MBfR zone" mixed; the bar's rotating speed was 325 revolution per minute (rpm). The water flowed upward through the "photo-zone" and left the reactor through effluent tubing at the top of the reactor. A table lamp of 875 lumen light intensity was set near the reactor beginning with stage 2 to provide light to the phytoplankton in the "photo-zone." To prevent the growth of the photosynthetic microorganisms in the "MBfR zone", it was blocked from the light by aluminum foil.

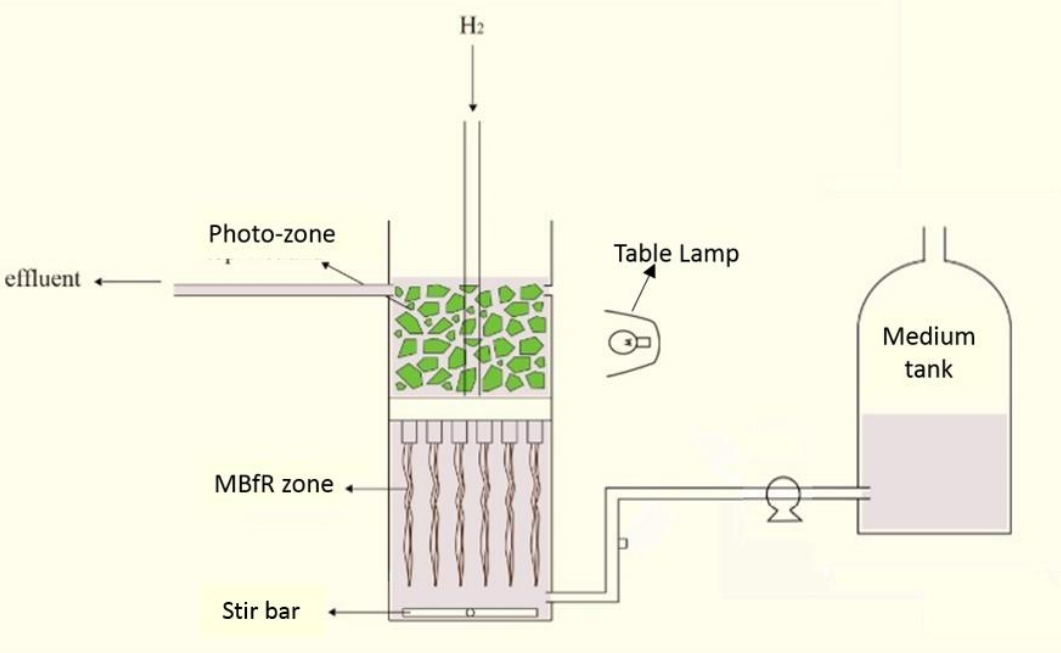

Figure 3. Experimental setup in the first 4 stages (without COD supply).

When organic matter was supplied to the bench-scale isMBfR, the experimental setup was modified by adding another medium tank (shown in Figure 4) to prevent denitrification in the medium tank. One medium tank--called contaminant tank--

contained the organic material and nitrate. The other medium tank –called the nutrient tank– contained nutrients (i.e., bicarbonate, trace minerals, and phosphate) to support the bacteria community in isMBfR. By separating contaminants and nutrients, bacteria did not accumulate to consume nitrate or COD in the medium tank. During the experiment, media from these two tanks were pumped with the same rate (half of the designed flow rate) and mixed before the influent.

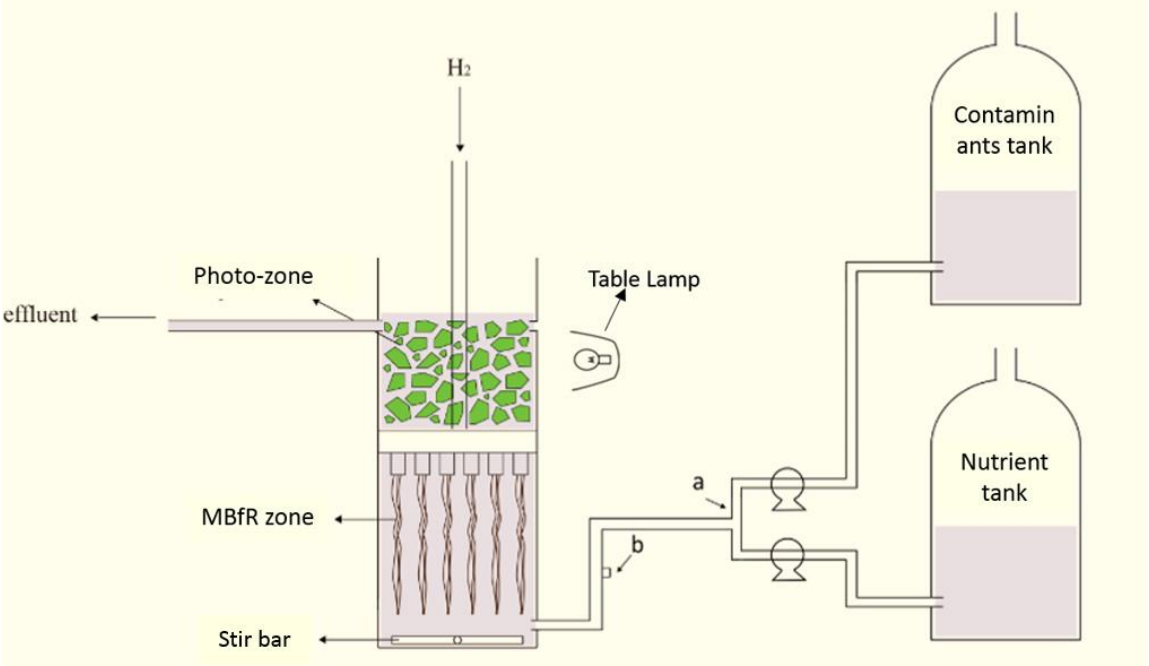

Figure 4. Experimental setup in stages 5, 6, and 7 (with COD supply)

2.2 Operating Conditions

Initially, the isMBfR was inoculated with 7 ml of activated sludge from the Mesa Northwest Wastewater Treatment Plant (Mesa, AZ, USA). After inoculation, H_2 was supplied to allow the formation of biofilm over the next 72 hours. Then, the synthetic water was pumped continuously into the reactor, and the first stage began. The chemical

composition of the synthetic water was, per liter: 0.087 g $NaNO_3$, 0.252 g $NaHCO_3$, 0.0053 g KH_2PO_4, 0.050 g $MgSO_4 \cdot 7H_2O$, and 1-ml trace mineral solution. The trace mineral solution contained, per liter: 100 mg $ZnSO_4 \cdot 7H_2O$, 30 mg $MnCl_2 \cdot 4H_2O$, 300 mg H_3BO_3, 200 mg $CoCl_2 \cdot 6H_2O$, 10 mg $CuCl_2 \cdot 2H_2O$, 10 mg $NiCl_2 \cdot 6H_2O$, and 30 mg Na_2SeO_3. In stages 5, 6, and 7, organic matter was supplied to the system. The composition of the organic matter was acetate, lactate, and citrate, and the percentages of COD from each were 41.9%, 37.6% and 20.5%, respectively. From stage 3, the pH of medium was adjusted to ~ 7.0 with 1 N sulfuric acid.

To evaluate the performance of a bench-scale isMBfR system, I conducted 7 stages with different operation conditions, summarized in Table 1.

Table 1. The operation conditions in the 7 stages

	Stage 1	Stage 2	Stage 3	Stage 4	Stage 5	Stage 6	Stage 7
H_2 pressure (psig)	14	12	15.5	15	15	15	0
Flow rate (L/d)	0.28	0.26	0.26	0.30	0.30	0.30	0.30
HRT (d)	2.1	2.3	2.3	2.0	2.0	2.0	2.0
Influent pH	-	8.4	6.97±0.07	6.99±0.09	7.03±0.06	7.13±0.05	7.29±0.03
Nitrate concentration in media (mg-N/L)	15	14.6	14.5	14.5	29	29	29
Nitrate concentration in influent (mg-N/L)	15.0±0.3	13.5±0.3	12.4±0.6	14.5±0.7	13.7±0.4	13.3±0.4	13.7±0.1
COD concentration in media (mg/L)	-	-	-	-	38.6	49.5	44.6
Influent COD concentration (mg/L)	-	-	-	-	10.2±1.8	14.7±1.1	11.9±0.4
Influent DO concentration (mg/L)	2.9	1.7	1.5	1.2	2.7	3.4	4.1

For the first 4 stages, the nitrate concentration was ~14.5 mg-N/L in the medium tank; the concentration was doubled in stages 5, 6, and 7 because two medium tanks were used. For the first 6 stages, the experimental H_2 pressure was adjusted so that excessive H_2 supply was avoided. Excess H_2 delivery was unwanted for three reasons. First, excess H_2 may lead to some safety problems in an open system. Second, without excess H_2 supply, the supplied H_2 can be considered completely utilized for denitrification, and the nitrate removal flux can be directly calculated by the H_2 supply flux. Third, excess H_2 supply may lead to unwanted sulfate reduction. In stage 7, H_2 supply was shut down to investigate the performance of isMBfR without H_2 supply.

In addition, after stage 2, the influent nitrate, DO, and COD concentrations always were lower than the concentrations in medium tanks due to biological activity in the influent tubing. Because this phenomenon could not be avoided completely for continuous operation, I measured the concentrations in the water just as it entered the isMBfR.

2.3 Water Sample Strategy and Analyses

During the experiments, I evaluated the performance of the "MBfR zone" and the "photo-zone." Figure 5 shows the locations of the sampling ports. For the "MBfR zone," I took samples at three different depths for measuring the nitrate, sulfate, nitrite, and COD concentrations; the goal was to evaluate whether or not the compartment was well mixed. I measured nitrate, sulfate, and nitrite concentrations daily in the first 3 stages and every two days from stages 4 to 7. I measured the COD concentration every two days in the influent at 3 different depths in stages 5, 6 and 7. Once I had proven that the liquid was well mixed in the "MBfR zone," I used one sample at "depth 2" to represent

the entire compartment. At steady state, when nitrate and COD concentrations were stable, I measured pH, alkalinity, and DO concentration in the influent and at "depth 2."

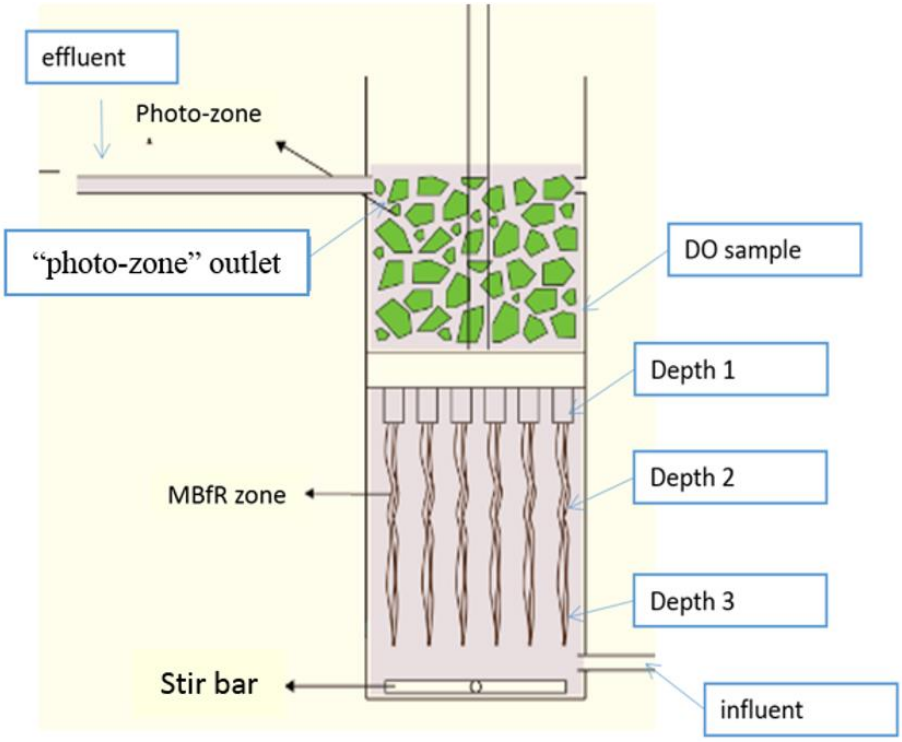

Figure 5. Locations of the sampling ports

For the "photo-zone," I took one sample from the outlet and one from the effluent tubing. I measured nitrate, sulfate, nitrite, and COD concentrations during the experimental period, and the sampling frequency was the same as the "MBfR zone." I measured pH and alkalinity at steady state. In addition, I measured the DO concentration in the bottom of the "photo-zone" at steady state.

Nitrate, sulfate, and nitrite concentrations were measured with an Ion Chromatograph (ICS-3000, Dionex Corp.) after filtering the samples through a 0.2-μm membrane filter (LC+PVDF membrane, Pall Life Sciences Acrodisc Syringe Filters).

COD concentrations were measure with a HACH COD kit with a range of 0-60 mg/L after being centrifuged in a speed of 13200 rpm for 10 minutes to remove suspended solids. I measured pH with a pH probe (Thermo Electron Corporation), alkalinity by a HACH alkalinity kit with a range of 25-400 mg $CaCO_3$/l. I measured the influent DO concentration through a HACH dissolved oxygen kit with a range of 0.3-15 mg/L and the DO concentration in MBfR zone and bottom of "photo-zone" with a HACH dissolved oxygen kit with a range of 0.1-1.0 mg/L. The DO measurements for the MBfR zone and the photo-zone were done in the anaerobic chamber.

2.4 Microbial Sampling and Analyses

I analyzed the microbial community through qPCR and light microscopy. I used qPCR to measure the cell abundance for general bacteria, denitrifying bacteria (DB), and sulfate-reducing bacteria (SRB). I utilized the light microscope to observe the photosynthetic microorganisms in "photo-zone" at the end of the entire experiment.

For qPCR, I took the microbial samples (in the "MBfR zone" and the "photo-zone") at the end of stages 2, 3, and 6 when the nitrate and COD concentrations were stable. I took the biofilm samples in the "MBfR zone" by cutting off a piece of fiber and sealing the remaining fiber with glue. I added 2 mL activated sludge after biofilm sampling to compensate for detachment of biofilm caused by sampling. I took the microbial samples in the "photo-zone" by taking one sponge cube out from this compartment, since the phototrophs are almost exclusively on the outside of the sponge cubes. I detached the biofilm from the fiber and sponge through the procedures described by Ontiveros et al. (2012). Then, I extracted the DNA with the DNeasy Blood and Tissue

Kit according to the manufacturer's directions and stored the DNA samples at -20℃ until qPCR test.

I established the standard curve for the plasmids containing target fragment with serial dilutions from 10^7 to 10^1 gene copies per μL as described in Ontiveros et al. (2012). I used the SYBR Premix Ex Taq Kit (Takara Bio, Inc, Japan) and performed the qPCR reaction in a 20-μL volume containing 10 μL of SYBR Premix Ex Taq Mix, 8.6 μL of H_2O, 0.2 μL of each forward and reverse primer (1 pmol/μL), and 1 μL of DNA template. Negative control utilized water instead of DNA templates, and I performed triplicate qPCR reactions for each sample and negative control.

Lastly, I converted gene copy numbers to cell numbers based on the following assumptions: one *nirK* gene and two *nirS* genes per bacterial cell for DB (Coates et al., 2001; Philippot, 2006), one *dsrA* gene per bacterial cell for SRB (Kondo et al., 2004), and 7 16S rRNA genes per bacterial cell (Fogel et al., 1999).

For light microscopy, I scratched the microbial samples from one sponge cube in the "photo-zone" at the end of stage 6. Then I gave the microbial samples to Alex Zevin (PhD student in the Swette Center for Environmental Biotechnology), and he observed the samples through the following procedures. The cells were imaged by light microscopy using an Olympus BX61 light microscope (Olympus Inc., Center Valley, PA) equipped with differential interference contrast (DIC) using a 60X oil-immersion objective. Fluorescent imaging was performed using an integrated mercury light source and a Cy5 filter. Images were captured with an Olympus DP72 color camera (Olympus Inc., Center Valley, PA).

CHAPTER 3

RESULTS AND PERFORMANCE OF THE BENCH SCALE ISMBFR SYSTEM

3.1 Experimental Results

In the first 4 stages, no organic matter was supplied to the system, making H_2 the only exogenous electron donor. Figure 6 summarizes the nitrate concentrations in the influent and effluent of the isMBfR during the first 4 stages. Generally, the effluent had a low nitrate concentration, below 4 mg-N/L. Although an apparent steady state was reached at the 5^{th} day of stage 1, nitrate removal increased at the end of this stage, and complete nitrate removal was achieved.

To avoid excess H_2, I lowered the H_2 pressure from 14 psig to 12 psig at the beginning of stage 2, which achieved 93% N removal. At the end of stage 2, I took a biofilm sample by cutting off a piece of fiber, and the biofilm was disturbed by this action. As a result, the nitrate concentration increased in the effluent (to ~ 2.7mgN/L), and I raised the H_2 pressure to 15.5 psig to recover the nitrate removal in stage 3. I took a biofilm sample at the end of stage 3.

Stage 4 had a relatively long duration (39 days) to ensure that the biofilm had enough time to recover from the disturbance caused by the biofilm sampling at the end of stage 3. In addition, I increased the flow rate by 15% to decrease the impact of nitrate reduction in the influent tubing. The effluent concentration spiked from the 61^{st} day to the 65^{th} day due to an accidental decrease of the H_2 pressure. After the pressure was corrected, the effluent nitrate concentration returned to its previous low level by the 68^{th} day.

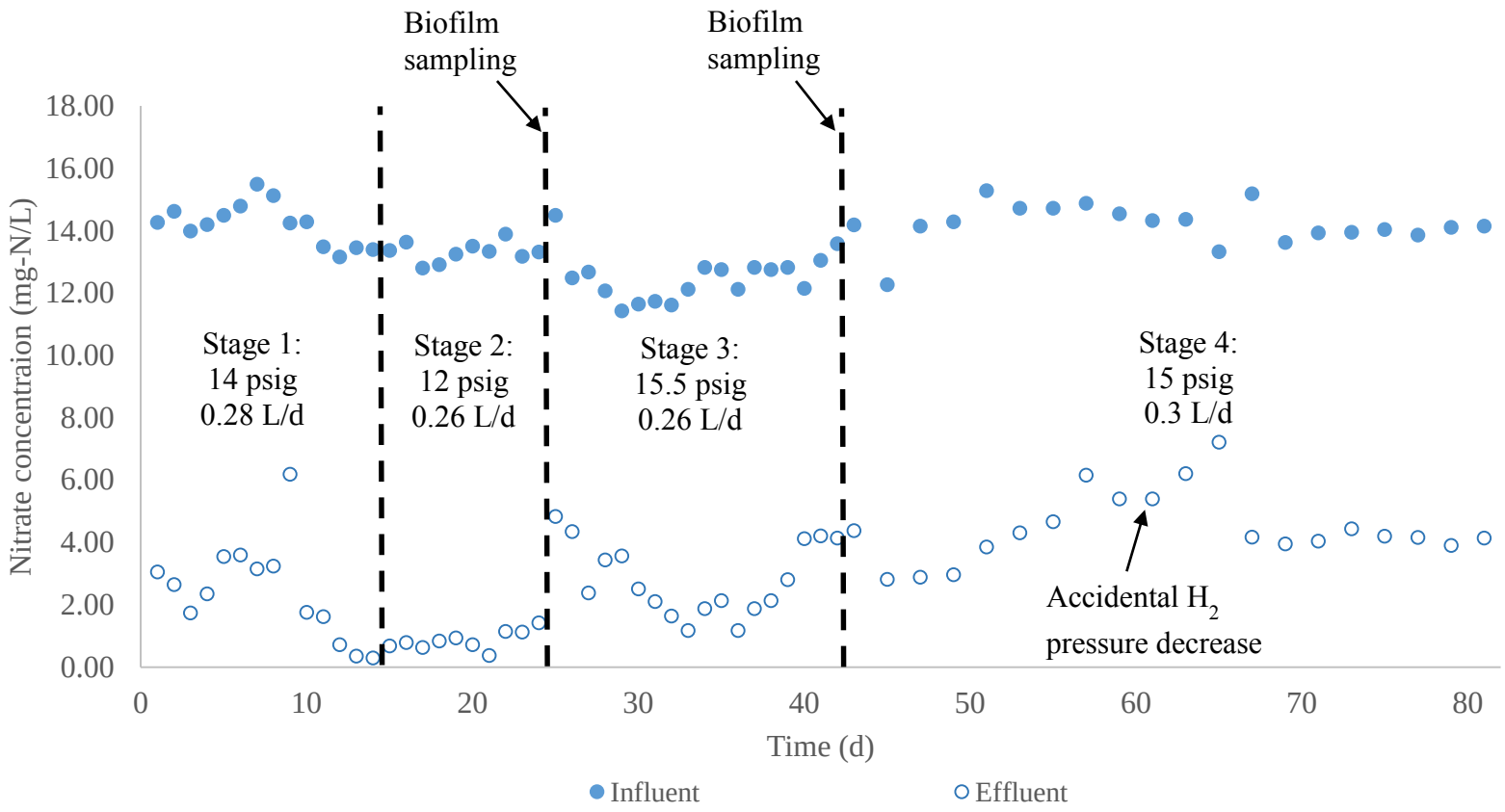

Figure 6. Nitrate concentration as a function of time in the first four stages, which had no input organic matter. H_2 pressure for the 4 stages were 14 psig, 12 psig, 15.5 psig, and 15 psig. The flow rates for the 4 stages were 0.28 mL/d, 0.26L/d, 0.26 L/d, and 0.3 L/d. Biofilm samples were taken at the end of stage 2 and stage 3 (24^{th} day and 39^{th} day). An accidental decrease of H_2 happened in 61^{st} day.

A relatively low concentration of organic matter (~ 10.2 mg COD/L) was supplied as an exogenous electron donor in stage 5. Then, the influent COD concentration was increased to ~14.7 mg COD/L in stage 6. Stage 7 had the same operating conditions as stages 5 and 6, except no H_2 supply and an influent COD concentration of ~11.9 mg COD/L.

The COD and nitrate concentrations in the influent and effluent are summarized in Figure 7. When H_2 was supplied as an electron donor (stages 5 and 6), the effluent nitrate concentration was kept at a low level (lower than 3 mg-N/L). Due to the extra electron donor in stage 6, the nitrate concentration in the effluent was lower than in stage 5. However, when H_2 supply was stopped, the effluent nitrate concentration returned to a high level (~12 mg-N/L). In all of these 3 stages, the effluent COD concentration was very low (< 2.5 mg COD/L), which indicates that heterotrophic bacteria were strongly active in denitrification and oxygen respiration.

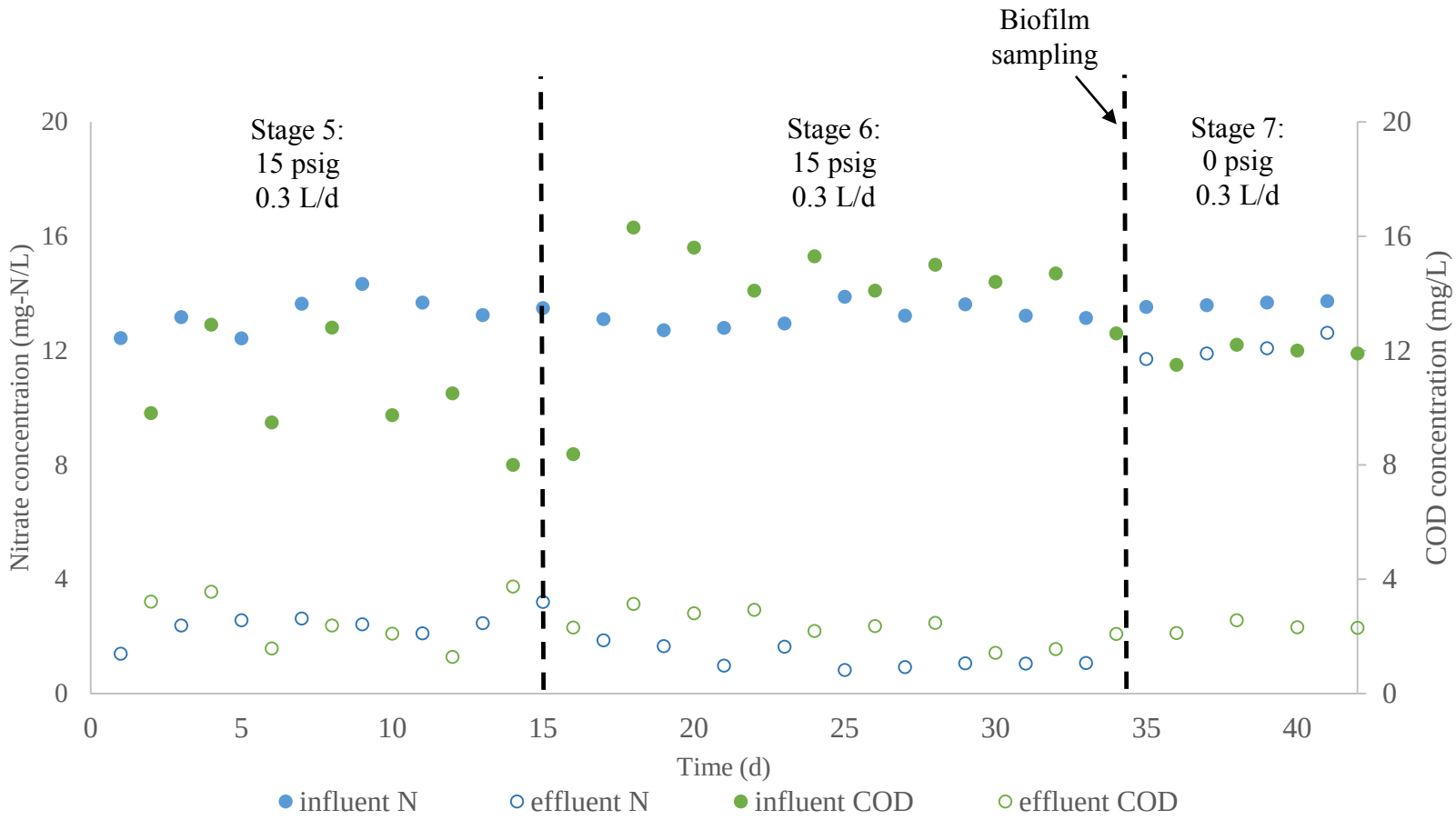

Figure 7. Nitrate and COD concentration as a function of time for stages 5 - 7, when COD was present in the influent. The H_2 pressure for these 3 stages were 15 psi, 15psi, and 0 psig; the flow rates for these 3 stages were 0.3 L/d. Biofilm sample was taken at the end of stage 6 (34^{th} day).

I measured nitrate, sulfate, and nitrite concentrations at the 3 different depths in the "MBfR zone," and the average value for each depth in each stage is summarized in Table 2. Nitrite concentrations are not shown because they were very low throughout the experimental period (lower than 0.3 mg-N/L). Concentrations of nitrate and sulfate were almost the same for each depth for each stage. Thus, the "MBfR zone" can be considered well mixed, with a concentration equal to the average value of the concentrations for the 3 depths.

Table 2. The nitrate and sulfate concentration for the 3 different depths of the "MBfR zone"

	Average nitrate concentration (mg-N/L)			Average sulfate concentration (mg/L)		
	Depth 1	Depth 2	Depth 3	Depth 1	Depth 2	Depth 3
Stage 1	2.9	2.9	2.9	24.3	25.0	25.1
Stage 2	2.0	1.9	2.0	22.2	22.2	22.3
Stage 3	2.8	2.9	2.9	34.4	34.1	34.1
Stage 4	4.7	4.9	4.8	38.2	38.3	38.1
Stage 5	2.6	2.7	2.7	43.6	43.7	44.0
Stage 6	1.1	1.1	1.1	52.4	52.2	52.2
Stage 7	12.5	12.4	12.4	39.1	38.4	38.5

I measured the soluble COD concentrations for the 3 different depths of "MBfR zone" in stages 5, 6, and 7, and the values are summarized in Table 3. The COD concentrations at the 3 depths of the "MBfR zone" also were close to each other, and I report the average COD concentration for each depth.

Table 3. COD concentrations for 3 depths in the "MBfR zone"

	Average COD concentration (mg/L)		
	Depth 1	Depth 2	Depth 3
Stage 5	3.4	2.6	3.2
Stage 6	2.1	2.2	2.2
Stage 7	1.4	1.1	1.4

Figures 8 and 9 summarize the average nitrate and sulfate concentrations at different locations of the reactor. "Influent" indicates the concentrations in the influent to the isMBfR, "MBfR zone" indicates the bulk concentrations in the "MBfR zone," "Photo-zone" refers to the concentrations in the outlet of the "photo-zone," and "Effluent" refers to the concentrations at the end of the effluent tubing. For nitrate, the concentration in the influent was much higher than for the other locations except during stage 7, which indicates that the isMBfR system brought about significant nitrate removal with H_2 supply. Nitrate concentrations in the "MBfR zone," the outlet of the "photo-zone", and the effluent were similar to each other. Based on the influent and effluent nitrate concentrations, the overall removal percentage of nitrate in the 7 stages were 79% ± 4%, 93% ± 2%, 79% ± 8%, 72.2% ± 8%, 81% ± 3%, 92% ± 3%, and 11% ± 2%. The high nitrate removal percentages for the first 6 stages indicate that the system worked well with or without COD input, but stage 7 had a poor removal percentage since the H_2 supply was ceased. For sulfate, the concentrations at the 4 locations were close to each other, which indicated that sulfate reduction was negligible in this system. Furthermore, I detected no evidence of sulfide odor. No sulfate reduction is the desired outcome.

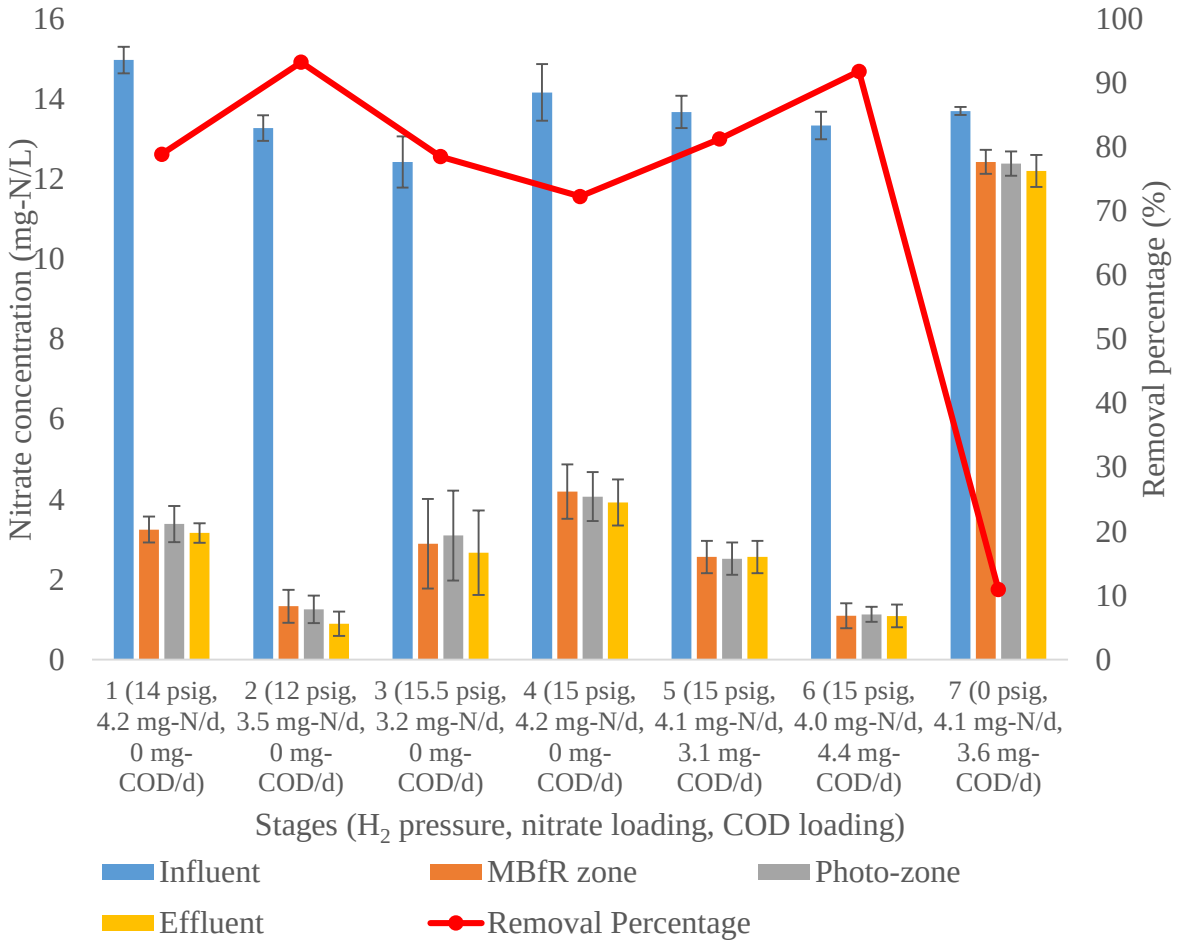

Figure 8. Nitrate concentrations at the different locations and the overall removal percentage. The H_2 pressure for the 7 stage were 14 psig, 12 psig, 15.5 psig, 15 psig, 15 psig, 15 psig, and 0 psig, respectively. The flow rates for the 7 stages were 0.28 mL/d, 0.26L/d, 0.26 L/d, 0.3 L/d, 0.3 L/d, 0.3 L/d, and 0.3 L/d, respectively. The influent NO_3^- concentration was approximately 14 mg-N/L for all stages.

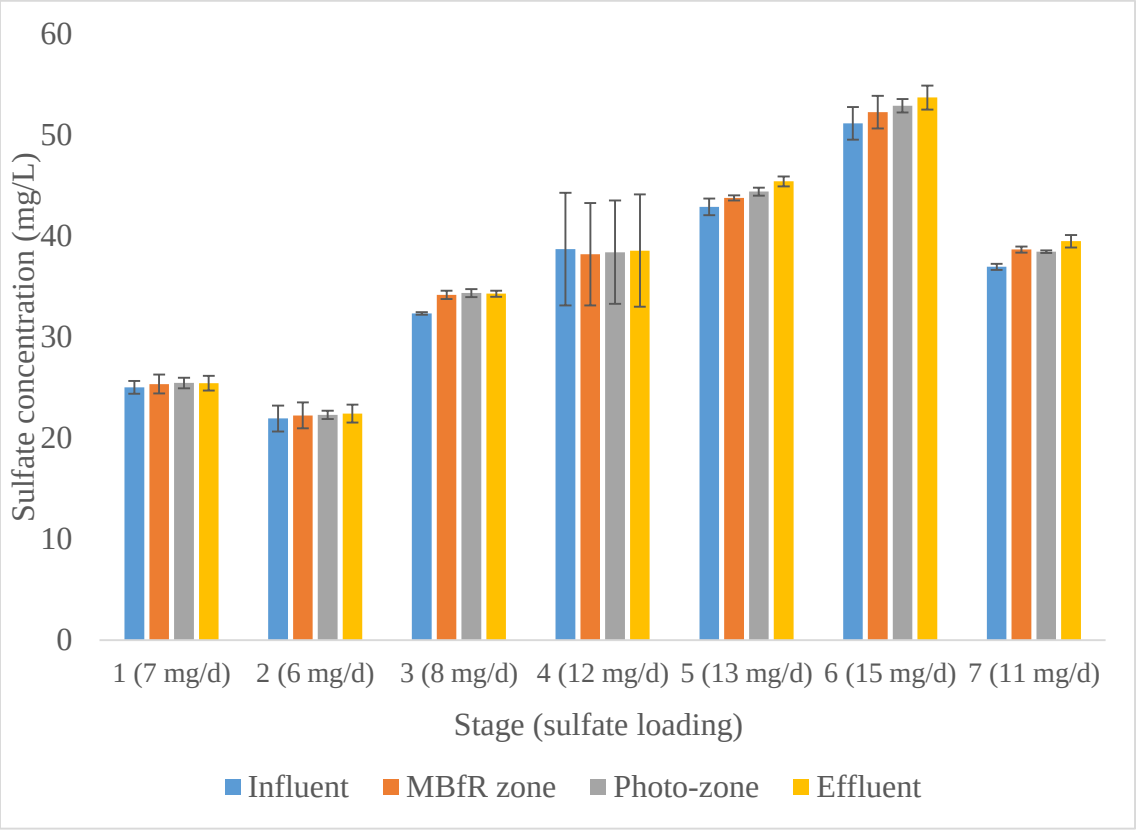

Figure 9. Sulfate concentrations for the different locations. Although the influent concentrations varied among the stages, the common result was that sulfate reduction was absent.

The COD concentrations for the different locations and the overall removal percentages are summarized in Figure 10. Similar to the results for nitrate, the influent had the highest COD concentration, and the other locations had similar COD concentrations. The COD removal percentages for stages 5, 6, and 7 were 75% ± 11%, 84% ± 4%, and 80% ± 1% respectively. The high COD removals support that an isMBfR system has high efficiency for organics removal, as well as nitrate removal. However, the organic matter used in this experiment was simple, and the nitrate supply exceeded the stoichiometric demand for COD. Although the effluent COD concentration was low, it was not zero. The most likely explanation for the incomplete COD removal is that the

soluble COD consisted of soluble microbial products (SMP) produced in the system (Hasar et al., 2008; Laspidou & Rittmann, 2002).

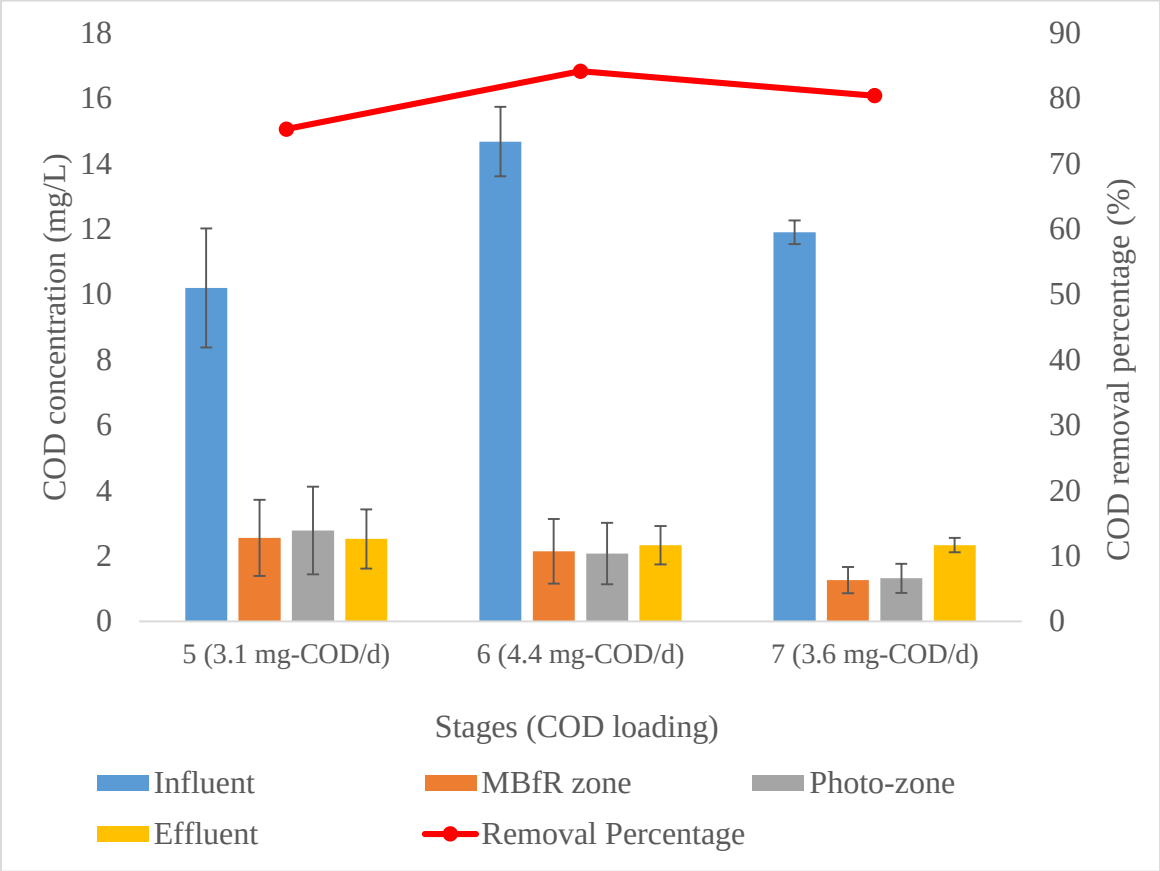

Figure 10. COD concentrations at the different locations and the overall removal percentage.

3.2 Nitrate and COD Removals in Different Compartments of the Reactor

I calculated the mass/time nitrate and COD removals (R, in mg-N/d for nitrate and mg-COD/d for COD) for the "MBfR zone" and "photo-zone," as well as for effluent tubing based on Eq. 5. Effluent tubing connected the outlet of "photo-zone" and removed effluent from the system.

$$R = Q \times (C_{in} - C_{out}) \quad Eq.(5)$$

Q is the volumetric flow rate (L/d), and C_{in} and C_{out} are the influent and effluent nitrate or COD concentrations for each compartment (mg-N/L for nitrate, mg-COD/L for COD).

The mass/time nitrate and COD removals are summarized in Tables 4 and 5. For nitrate, stage 6 had the highest overall mass/time nitrate removal due to the high H_2 pressure (15 psig) and COD supply, while stage 7 had the lowest overall mass/time nitrate removal, since H_2 was no longer supplied. For COD, the mass/time COD removal corresponded to the COD loading; thus, stage 6 had the highest mass/time COD removal (3.7 mg COD/d).

Compared with the "photo-zone" and effluent tubing, the majority of the denitrification occurred in the "MBfR zone," which indicates that the isMBfR was the core of denitrification for this bench-scale system. With H_2 supply (first 6 stages), a high nitrate removal (all over 2.5 mgN/d) was achieved. Once the H_2 supply was ceased (stage 7), the nitrate removal dropped drastically from 3.7 mg-N/d (stage 6) to 0.5 mg-N/d, indicating that H_2 was the primary electron donor in this system. Since the role for isMBfR module is to deliver H_2 to the wetland for denitrification, the results supported the concept that isMBfR can augment the nitrate removal capacity of constructed wetland.

Nitrate removal in the "photo-zone" was negligible throughout the experiment. In theory, the "photo-zone" could contribute to nitrate removal through heterotrophic denitrification. The most likely explanation for the trivial nitrate removal is the lack of electron donor, as the majority of electron donors were consumed in "MBfR zone." For

the same reason, denitrification in the effluent tubing also was insignificant. In addition, since the majority of COD was removed in the "MBfR zone," a low COD concentration (below 2.5 mg/L) entered the "photo-zone" and effluent tubing, which led to a low COD removal (nearly 0 mg/d) in both compartments.

Table 4. Mass/time nitrate removal contributed by each compartment of the reactor

Stages (H_2 pressure, nitrate loading, COD loading)	Mass/time nitrate removal (mg-N/d)			
	MBfR zone	Photo-zone	effluent tubing	overall
1 (14 psig, 4.2 mg-N/d, 0 mg-COD/d)	3.3	0.0	0.1	3.4
2 (12 psig, 3.5 mg-N/d, 0 mg-COD/d)	3.1	0.0	0.1	3.2
3 (15.5 psig, 3.2 mg-N/d, 0 mg-COD/d)	2.5	-0.1	0.1	2.5
4 (15 psig, 4.2 mg-N/d, 0 mg-COD/d)	3.0	0.0	0.0	3.0
5 (15 psig, 4.1 mg-N/d, 3.1 mg-COD/d)	3.3	0.0	0.0	3.3
6 (15 psig, 4.0 mg-N/d, 4.4 mg-COD/d)	3.7	0.0	0.0	3.7
7 (0 psig, 4.1 mg-N/d, 3.6 mg-COD/d)	0.4	0.0	0.1	0.5

Table 5. Mass/time COD removal contributed by each compartment of the reactor

Stages (COD loading)	Mass/time COD removal (mg/d)			
	MBfR zone	Photo-zone	effluent tubing	overall
5 (3.1 mg-COD/d)	2.3	-0.2	0.1	2.2
6 (4.4 mg-COD/d)	3.8	0.0	-0.1	3.7
7 (3.6 mg-COD/d)	3.2	0.0	-0.3	2.9

3.3 pH, DO and Alkalinity in Steady-State

Table 6 summarizes the pH, alkalinity, and DO at steady state for stages 2-7. For stages 3–6, although the influent pH was adjusted to ~7.0, high pH still was observed in the "MBfR zone" (around 9.0) and the "photo-zone" (around 9.1). Lee and Rittmann (2003) recommended an optimal pH range of 7.7-8.6 for autotrophic denitrifiers and indicated that high pH may favor the formation of nitrite. However, the isMBfR maintained high denitrification efficiency with negligible nitrite formation throughout the experimental period. Stage 7 had a much lower pH in the "MBfR zone," the "photo-zone," and the effluent, which agrees with the lower nitrate removal in this stage.

Alkalinity was measured beginning with stage 4. Alkalinity significantly increased in the "MBfR zone" due to denitrification taking place in this compartment. Denitrification is a major alkalinity source for MBfR through the consumption of protons (H^+) and production of bicarbonate. As a consequence, the lowest alkalinity for stage 7 in "MBfR zone" corresponded to the lowest nitrate removal in this stage. Alkalinity hardly changed in the "photo-zone" and effluent tubing due to the trivial denitrification in these two compartments.

Due to biological activity in the influent tubing, the influent DO concentration was low (below 4.1 mg/L). The DO concentration was negligible in "MBfR zone" (Table 4) and also very low at the bottom of "photo-zone" (less than 1.0 mg/L). The latter finding implies that oxygen entering the "MBfR zone" from the "photo-zone" was not large. Phytoplankton (such as cyanobacteria) accumulated in the "photo-zone" produced oxygen through photosynthesis, and the effluent DO was around 4 mg/L. Nevertheless, the DO concentration at the bottom of the "photo-zone" was low. Possible explanations are that the production of oxygen was small, that advection transported the DO to the top of the 'photo-zone," and that the DO was completely consumed by bacterial respiration.

Table 6. Steady-state pH, alkalinity and DO at different locations in the isMBfR

	pH				Alkalinity (mg CaCO3/l)				DO (mg/L)		
Stage	Influent	MBfR zone	Photo-zone	Effluent	Influent	MBfR zone	Photo-zone	Effluent	Influent	MBfR zone	Bottom of photo-zone
2	8.4	9.1	9.1	8.9	-	-	-	-	1.7	<0.1	<0.1
3	6.97±0.07	9.03±0.06	8.97±0.02	8.89±0.11	-	-	-	-	1.5	<0.1	<0.1
4	6.99±0.09	8.86±0.14	8.91±0.15	8.57±0.18	129±7	161±9	163±6	165±6	1.2	<0.1	<0.1
5	7.03±0.06	9.02±0.08	9.10±0.1	8.80±0.08	134±4	177±2	181±6	190±7	2.7	<0.1	<0.1
6	7.13±0.05	9.20±0.05	9.26±0.04	8.92±0.13	134±4	183±3	186±3	188±3	3.4	<0.1	<0.1
7	7.29±0.03	7.91±0.08	8.06±0.07	7.98±0.05	140±3	152±1	157±3	155±2	4.1	0.8	1.0

3.4 Conclusion

Removals of nitrate and COD were good in the bench-scale isMBfR except in stage 7, during which the H_2 supply was shut down. Thus, H_2 was the primary electron donor in this system. The "MBfR zone" contributed essentially all nitrate removal, which reinforces the principle that the H_2-based MBfR can augment the nitrate removal capacity for a constructed wetland. Sulfate reduction and nitrite formation were trivial throughout the experiment, which indicates that no deleterious products were produced when the isMBfR was properly managed. Denitrification increased the alkalinity and pH in the "MBfR zone," but the high pH had no negative impact on the performance of isMBfR.

CHAPTER 4

MODELING THE NITRATE REMOVAL CAPACITY OF THE ISMBFR THROUGH THE STOICHIOMETRIC RELATIONSHIPS AMONG H_2, NITRATE, OXYGEN, COD, AND ALKALINITY

Stoichiometry provides us mathematical relationships among the electron donors and electron acceptors involved in the isMBfR system. Thus, in theory, stoichiometry can enable us to model the nitrate removal capacity of an isMBfR system based on other parameters (e.g., flow rate, COD loading, and H_2 pressure).

To test this hypothesis, I derived mathematical relationships among H_2, nitrate, dissolved oxygen, COD, and alkalinity, and I estimated the nitrate-removal capacity for each stage based on the stoichiometric relationships. Without COD supply (first 4 stages), I estimated the nitrate removal capacity based on the relationship between H_2 delivery and nitrate + O_2 loading. With COD supply (stages 5-7), I estimated the mass/time nitrate removal capacity based on stoichiometric relationships among COD and nitrate + O_2 loadings and H_2-delivery capacity. I also estimated the mass/time nitrate removal based on relationships between nitrate and alkalinity as an alternative method for modeling the nitrate removal capacity. Finally, I compared the estimated nitrate removal capacities with the experimental nitrate removals.

4.1 Derivation of the Stoichiometric Relationships

4.1.1 Relationship between Nitrate and H_2

According to Tang et al. (2012), the maximum delivery capacity flux of H_2 can be estimated based on the H_2 pressure:

$$J_{m,max} = \frac{K_m}{z_m} P_0 k_1 \frac{d_m - z_m}{z_m} \quad Eq.(6)$$

Plugging the parameters for polypropylene fibers (Tang et al., 2012) into Eq. 6 gives:

$$J_{m,max} = 0.0145 \times P \quad Eq.(7)$$

$J_{m,max}$ is the maximum delivery capacity flux of H_2 (g/m^2-d), and P is the H_2 pressure (psig). This equation provides us the maximum H_2 flux that could be delivered by the membrane fibers.

For the first 4 stages, H_2 was oxidized by respirations of nitrate and O_2; then, the H_2 flux used for denitrification should be the total H_2 flux ($J_{m,max}$) after subtracting the H_2 flux utilized for oxygen respiration. The later flux can be calculated by:

$$J_{O_2} = \frac{Q(S_{DO}^0 - S_{DO})}{A_M} \times \frac{1g}{1000mg} = \frac{Q\Delta S_{DO}}{A_M} \times \frac{1g}{1000mg} \quad Eq.(8)$$

A_M is the membrane surface area (m^2), J_{O_2} is the O_2 removal flux (g/m^2-d), S_{DO}^0 is the influent DO concentration (mg/L), S_{DO} is the bulk concentration for DO in "MBfR zone" (mg/L), and ΔS_{DO} is the difference between influent and bulk DO concentration (mg/L).

The relationship between H_2 and O_2 can be derived from the stoichiometry in Eq. (9):

$$\frac{1}{4}O_2 + \frac{1}{2}H_2 \rightarrow \frac{1}{2}H_2O \quad Eq.(9)$$

from which I converted the O_2 removal flux to the H_2 flux for O_2 respiration ($J_{O_2-H_2}$, in g-H_2/m^2-d) using Eq. (8):

$$J_{O_2-H_2} = \frac{2 \times 2g-H_2/mole}{32g-O_2/mole} \times J_{O_2} = 0.125 \times \frac{Q(S_{DO}^0 - S_{DO})}{A_M} \times \frac{1g}{1000mg}$$

$$= 0.125 \times \frac{Q\Delta S_{DO}}{A_M} \times \frac{1g}{1000mg} \quad Eq.(10)$$

Then, the H_2 flux for nitrate removal ($J_{NO_3-H_2}$, in g-H_2/m^2-d) can be calculated from:

$$J_{NO_3-H_2} = \mathrm{J_{m,max}} - J_{O_2-H_2} = 0.0145P - 0.125 \times \frac{Q\Delta S_{DO}}{A_M} \times \frac{1g}{1000mg} \quad \text{Eq.}(11)$$

The next step is to convert the H_2 flux for nitrate removal to nitrate-removal flux through the stoichiometry. To build the biochemical relationships between nitrate and H_2, I assumed that the percentage of electron donor for cell synthesis (f_s) ranged from 0 to 0.25 (Rittmann & McCarty, 2001). $f_s = 0$ means no biomass formation in the denitrification process, while $f_s = 0.25$ indicates a maximum percentage of biomass formation in an autotrophic denitrification process (Rittmann & McCarty, 2001). Then, the biochemical equations are described by Eqs. 12 and 13:

$f_s = 0$ (no biomass formation):

$$0.2NO_3^- + 0.2H^+ + 0.5H_2 = 0.1N_2 + 0.6H_2O \quad \text{Eq. (12)}$$

$f_s = 0.25$ (max biomass formation):

$$0.159NO_3^- + 0.159H^+ + 0.5H_2 + 0.045CO_2 = 0.55H_2O + 0.009C_5H_7O_2N + 0.075N_2 \quad \text{Eq. (13)}$$

Based on the stoichiometry of Eqs. 12 and 13, I can convert H_2 flux (g/m^2-d) for nitrate to nitrate removal flux (g-N/m^2-d) by Eqs. 14 and 15:

$f_s = 0$ (no biomass formation):

$$J_{NO_3-est} = \frac{J_{NO_3-H_2}}{0.357} \quad Eq.(14)$$

f_s = 0.25 (max biomass formation):

$$J_{NO_3-est} = \frac{J_{NO_3-H_2}}{0.45} \qquad Eq.(15)$$

J_{NO_3-est} is the estimated nitrate removal flux (g-N/m^2-d).

When f_s = 0, all H_2 is used for nitrate reduction, and this gives the maximum nitrate-removal flux for a certain H_2 supply; thus, Eq. 14 estimates the maximum estimated nitrate-removal flux. When f_s = 0.25, the minimum percentage of H_2 is used for nitrate reduction, because some of the H_2 is used for reducing CO_2 and NO_3^- for biomass synthesis. Thus, Eq. 15 estimates the minimum nitrate removal flux for a certain H_2 flux.

Next, by plugging Eq. 11 into Eqs. 14 and 15, I calculated the maximum nitrate removal fluxes (J_{NO_3-est}, in g-N/m^2-d), which are shown in Eqs. 16 and 17:

f_s is 0 (max estimated nitrate removal flux):

$$J_{NO_3-est} = \frac{(0.0145P - 0.125 \times \frac{Q\Delta S_{DO}}{A_M} \times \frac{1g}{1000mg})}{0.357} \quad Eq.(16)$$

f_s is 0.25 (min estimated nitrate removal flux):

$$J_{NO_3-est} = \frac{(0.0145P - 0.125 \times \frac{Q\Delta S_{DO}}{A_M} \times \frac{1g}{1000mg})}{0.45} \quad Eq.(17)$$

Finally, I calculated the experimental nitrate removal flux (J_{NO_3-exp}, in g-N/m^2-d) through Eq. 18:

$$J_{NO_3-exp} = \frac{Q(S^0_{nitrate} - S_{nitrate})}{A_M} \times \frac{1g}{1000mg} = \frac{Q\Delta S_{nitrate}}{A_M} \times \frac{1g}{1000mg} \quad Eq.(18)$$

$S^0_{nitrate}$ is influent nitrate concentration (mg-N/L), $S_{nitrate}$ is the bulk concentration for nitrate in "MBfR zone" (mg-N/L), $\Delta S_{nitrate}$ is the difference between influent and bulk concentration of nitrate (mg-N/L).

Table 7 summarizes the parameters needed for the calculations in stages 1 – 4.

Table 7. Parameters for the calculations of experimental and estimated nitrate removal flux.

	H_2 pressure (psig)	Surface area (m^2)	Flow rate (L/d)	$\Delta S_{nitrate}$ (mg-N/L)	ΔS_{DO} (mg/L)
Stage 1	14	0.07	0.28	11.7	2.9
Stage 2	12	0.07	0.26	11.9	1.7
Stage 3	15.5	0.07	0.26	9.5	1.5
Stage 4	15	0.07	0.3	10.0	1.2

4.1.2 Relationships among COD, Nitrate, Dissolved Oxygen, and H_2

In Stages 5, 6, and 7, which had COD supplied, denitrification could be driven by COD oxidation, as well as by H_2 oxidation. As the operating conditions for stages 5 and 6 were the same as stage 4, except for the COD supply, the mass/time nitrate removals contributed by H_2 for these two stages were the same as for stage 4, which was 3 mg-N/d (shown in Table 4). For stage 7, without H_2 supply, no nitrate would be removed by H_2. Since the heterotrophs tended to be present in the bulk liquid and the outer layer of the biofilm, I assumed that the heterotrophs would consume dissolved oxygen first.

I now derive the relationship between nitrate and COD through stoichiometry. I assumed that the percentage of electron donor for cell synthesis (f_s) ranged from 0 to 0.52 for heterotrophic denitrification (Rittmann & McCarty, 2001). Again, $f_s = 0$ means no biomass formation during heterotrophic denitrification, while $f_s = 0.52$ indicates a

maximum percentage of biomass formation during the heterotrophic denitrification. Then, I built the biochemical equations for nitrate and the 3 organic materials utilized in this experimental, as shown in Eqs. 19 - 24:

$f_s = 0$ (no biomass formation):

Acetate:

$$0.125CH_3COO^- + 0.2NO_3^- + 0.2H^+ = 0.1N_2 + 0.125CO_2 + 0.125HCO_3^- + 0.125H_2O \quad \text{Eq. (19)}$$

Lactate:

$$0.0.0833C_3H_5O_3^- + 0.2NO_3^- + 0.2H^+ = 0.1N_2 + 0.1667CO_2 + 0.0833HCO_3^- + 0.27H_2O \quad \text{Eq. (20)}$$

Citrate:

$$0.0556C_6H_5O_7^{3-} + 0.2NO_3^- + 0.2H^+ = 0.1N_2 + 0.1667CO_2 + 0.1667HCO_3^- + 0.156H_2O \quad \text{Eq. (21)}$$

$f_s = 0.52$ (max biomass formation):

Acetate:

$$0.125CH_3COO^- + 0.1146NO_3^- + 0.115H^+ = 0.0186C_5H_7O_2N + 0.048N_2 + 0.0312CO_2 + 0.125HCO_3^- + 0.117H_2O \quad \text{Eq. (22)}$$

Lactate:

$$0.0833C_3H_5O_3^- + 0.1146NO_3^- + 0.115H^+ = 0.0186C_5H_7O_2N + 0.048N_2 + 0.0738CO_2 + 0.0833HCO_3^- + 0.159H_2O \quad \text{Eq. (23)}$$

Citrate:

$$0.0556C_6H_5O_7^{3-} + 0.1146NO_3^- + 0.115H^+ = 0.0186C_5H_7O_2N + 0.048N_2 + 0.0738CO_2 + 0.1667HCO_3^- + 0.048H_2O \quad \text{Eq. (24)}$$

Based on the stoichiometry obtained from Eqs. 19 - 24, I calculated the COD removed by nitrate respiration (R_{COD-N}, in mg-N/d) using Eqs. 25 and 26:

$f_s = 0$ (no biomass formation):

$$R_{COD-N} = \frac{Q \times ((S^0_{COD} - S_{COD}) - \Delta S_{DO})}{2.86} = \frac{Q \times (\Delta S_{COD} - \Delta S_{DO})}{2.86} \quad Eq.(25)$$

$f_s = 0.52$ (max biomass formation):

$$R_{COD-N} = \frac{Q \times ((S^0_{COD} - S_{COD}) - \Delta S_{DO})}{5} = \frac{Q \times (\Delta S_{COD} - \Delta S_{DO})}{5} \quad Eq.(26)$$

S^0_{COD} and S_{COD} are the influent and bulk COD concentrations for "MBfR zone" (mg/L), and ΔS_{COD} is the difference between the influent and bulk COD concentration of "MBfR zone" (mg/L).

When $f_s = 0$, the entire COD is utilized to reduce nitrate, and a certain COD oxidation achieves the maximum nitrate reduction. When $f_s = 0.52$, the minimum percentage of COD is used for nitrate reduction, since some is used to reduce NO_3^- for synthesis; thus, a certain COD oxidation removes the minimum nitrate.

I estimated the total estimated mass/time nitrate removal ($R_{T,N}$, in mg-N/d) by summing up the COD removed nitrate and the H_2 removed nitrate (R_{H_2-N}, in mg-N/d), as shown in Eqs. 27 and 28:

f_s = 0 (max estimated nitrate removal):

$$R_{T,N} = R_{COD-N} + R_{H_2-N} = \frac{Q \times (\Delta S_{COD} - \Delta S_{DO})}{2.86} + R_{H_2-N} \quad Eq.(27)$$

f_s = 5.2 (min estimated nitrate removal):

$$R_{T,N} = R_{COD-N} + R_{H_2-N} = \frac{Q \times (\Delta S_{COD} - \Delta S_{DO})}{5} + R_{H_2-N} \quad Eq.(28)$$

Finally, I assessed the estimated mass/time nitrate removal with COD supply by comparing it with the experimental mass/time nitrate removal (in Table 4). Table 8 summarizes the parameters needed for the calculations for stages 5, 6, and 7.

Table 8. Parameters for the estimation of mass/time nitrate removal.

	H_2-removed nitrate (mg-N/d)	Flow rate (L/d)	ΔS_{DO} (mg/L)	ΔS_{COD} (mg/L)
Stage 5	3.0	0.3	2.7	7.7
Stage 6	3.0	0.3	3.4	12.5
Stage 7	0.0	0.3	3.3	10.6

4.1.3 Relationship between Nitrate and Alkalinity

Denitrification increases the alkalinity by consuming protons (H^+). Thus, the change of nitrate can be related to the change of alkalinity through stoichiometry. In this section, I derive the equations that describe the relationship between mass/time nitrate removal and the change of alkalinity.

The biochemical equations in the previous sections show the relationship between nitrate and protons: 1 mole of nitrate reduction consumes 1 mole of protons. This relationship enables me to calculate the change of alkalinity, as shown in Eq. 29:

$$\Delta[Alk] = \Delta[H^+] \qquad \text{Eq. (29)}$$

$\Delta[Alk]$ is the change of alkalinity in the "MBfR zone" (mM), $\Delta[H^+]$ is the change of H^+ in the "MBfR zone" (mM). By substituting $\Delta[H^+]$ with nitrate removal, I obtain Eq. 30:

$$\Delta[Alk] = \frac{R_{A,N}}{Q \times 14 \frac{mg-N}{mMole}} \qquad Eq. (30)$$

$R_{A,N}$ is the estimated mass/time nitrate removal through the alkalinity and COD changes (mg-N/d).

By rewriting Eq. 31, I can estimate the mass/time nitrate removal by alkalinity change through Eq. 31:

$$R_{A,N} = Q \times 14 \frac{mg-N}{mMole} \times \Delta[Alk] \quad Eq. (31)$$

Then, I evaluated the estimated mass/time nitrate removal by comparing it with the experimental nitrate removal (in Table 4), and Table 9 summarizes the parameters utilized for the calculations.

Table 9. Parameters for the estimation of mass/time nitrate removal through alkalinity change.

	Flow rate (L/d)	ΔAlk (mg $CaCO_3$/L)	Δ[Alk] (mM)
Stage 4	0.3	32	0.64
Stage 5	0.3	43	0.86
Stage 6	0.3	50	1.00
Stage 7	0.3	12	0.24

4.2 Assessment of Estimated Nitrate Removal Capacities in "MBfR Zone"

4.2.1 Without COD Supply (First 4 Stages)

For the first 4 stages, I calculated the estimated nitrate-removal flux based on Eqs. 16 and 17 and the experimental nitrate removal flux based on Eq. 18. The experimental and estimated nitrate removal fluxes are compared in Figure 11.

If the H_2-delivery capacity is not in excess, all H_2 supplied should be completely consumed for denitrification, along with O_2 respiration. In theory, I can convert the H_2-delivery flux to nitrate-removal flux through stoichiometry and considering H_2 consumption for O_2 reduction. The experimental nitrate-removal flux should lie between the minimum and maximum estimated nitrate removal fluxes I computed from the stoichiometry. According to Figure 11, the experimental nitrate removal flux lay between the minimum and maximum estimated nitrate-removal fluxes in stages 1, 2, and 4. This supports that the nitrate removal capacity of an isMBfR can be successfully estimated by stoichiometry when H_2 is the only electron donor. It also implies that f_s was between 0 and 0.25.

The experimental nitrate removal flux in stage 3 was lower than the minimum estimated nitrate-removal flux. This means that the H_2 supply capacity was in excess of the demand for nitrate removal, and more nitrate reduction was possible. However, since nitrate still was present in the effluent (an average concentration of 2.7 mg-N/L) and sulfate reduction did not occur, the actual H_2 demand was less than the H_2 delivery capacity due to insufficient biofilm or possible mass-transport of NO_3^- into the biofilm.

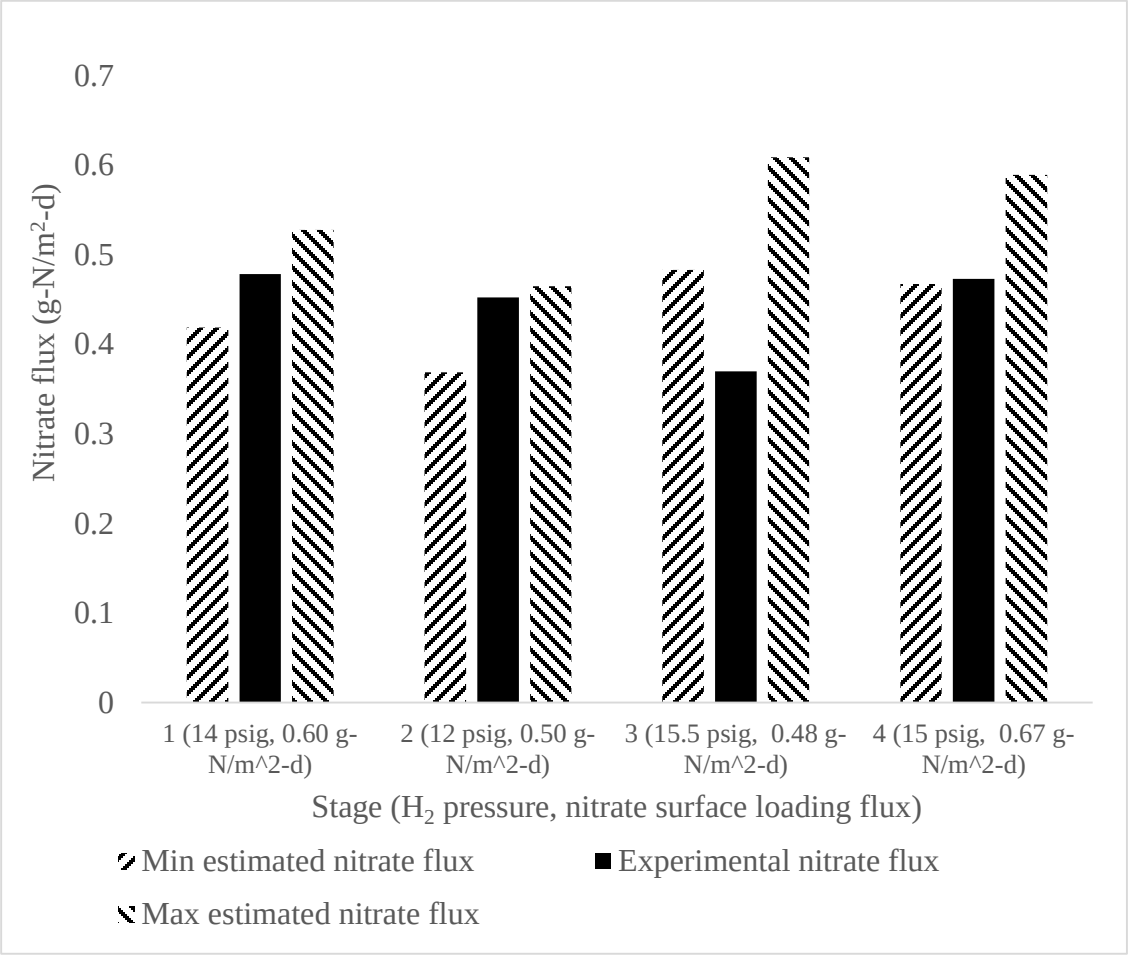

Figure 11. The comparison among experimental nitrate removal flux, max and min estimated nitrate removal flux. The H_2 pressure and flow rate for each stage are shown in Table 7.

4.2.2 With COD Supply (Stages 5, 6, and 7)

For stages 5, 6, and 7, I estimated the mass/time nitrate removal based on Eqs. 27 and 28. The estimated mass/time nitrate removals are compared with the experimental mass/time nitrate removal in Figure 12. For stages 6 and 7, the experimental mass/time nitrate removal of all the 3 stages lay between the minimum and maximum estimated mass/time nitrate removal, which indicates that the combined supply of COD and H_2 was

sufficient to completely reduce NO_3^- and O_2. The oxidation of COD means that the autotrophic denitifiers consumed less H_2 than in stages with no COD addition. With COD supplied, heterotrophic denitrifiers accumulated in the "MBfR zone," presumably on the membrane fibers, since virtually all denitrification took place in that zone. It is possible that the heterotrophs competed for space with the autotrophic denitrifiers, but any negative impact was small, since NO_3^- removal was nearly complete in stages 6 and 7.

In Stage 7, the experimental NO_3^- removal, solely from heterotrophic oxidation of COD, corresponded to the minimum estimated removal based on COD removal. This implies that f_s was close to its maximum value for heterotrophs, 0.52. This is consistent with net growth of heterotrophs in stage 7 as they became more important for denitrification due to the loss of autotrophic denitrification. However, the total removal of NO_3^- was much less in stage 7 due to the limited amount of COD available to drive denitrification.

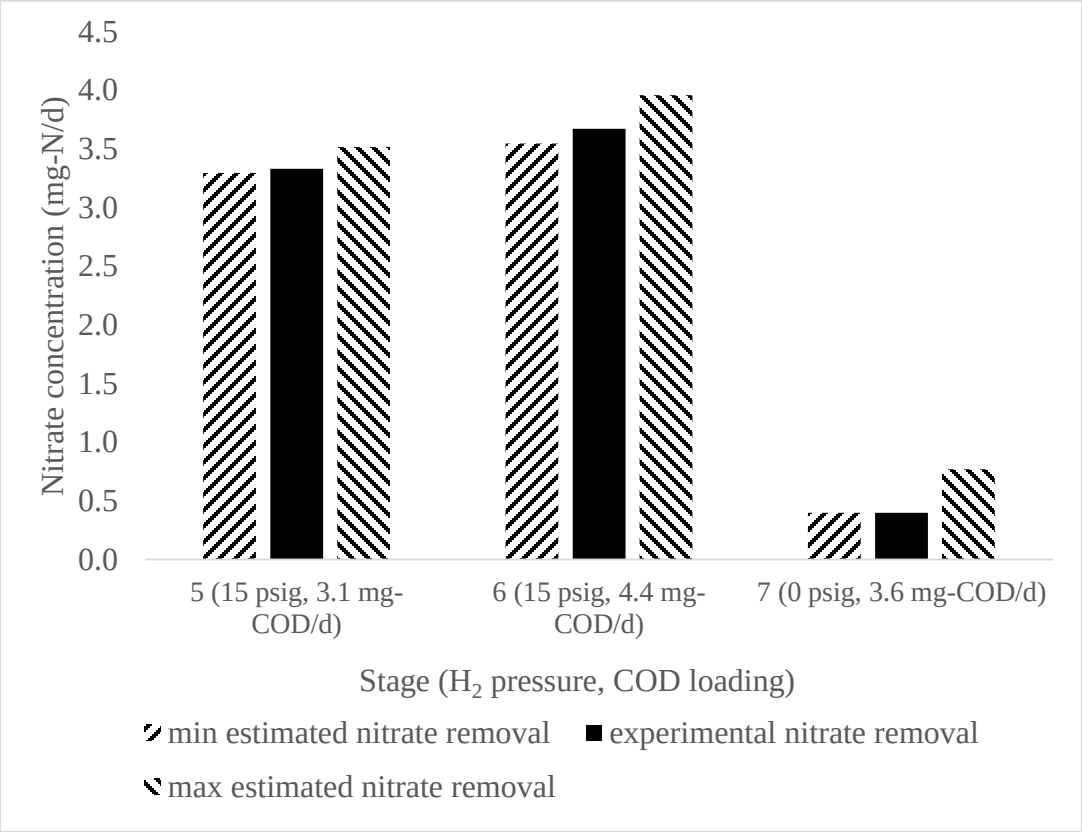

Figure 12. Comparison among experimental mass/time nitrate removal, min and max estimated mass/time nitrate removal. The H_2 pressure and flow rate for each stage are shown in Table 8. The estimated mass/time nitrate removal was the sum of nitrate removal capacities for COD and H_2.

4.2.3 Evaluation of the Nitrate Removal Estimated through the Relationship between Alkalinity and Nitrate

Based on Eq. 31, I estimated the mass/time nitrate removal by the alkalinity changes. Figure 13 shows comparison between the estimated and experimental mass/time nitrate removal. For all of the 4 stages I could evaluate (stages 4 through 7), the difference between the estimated and experimental mass/time nitrate removal was small. This provides us an alternative way to estimate the nitrate removal performance

for an isMBfR system. However, since we need the alkalinity change, we can only use this method during the operation period of an isMBfR.

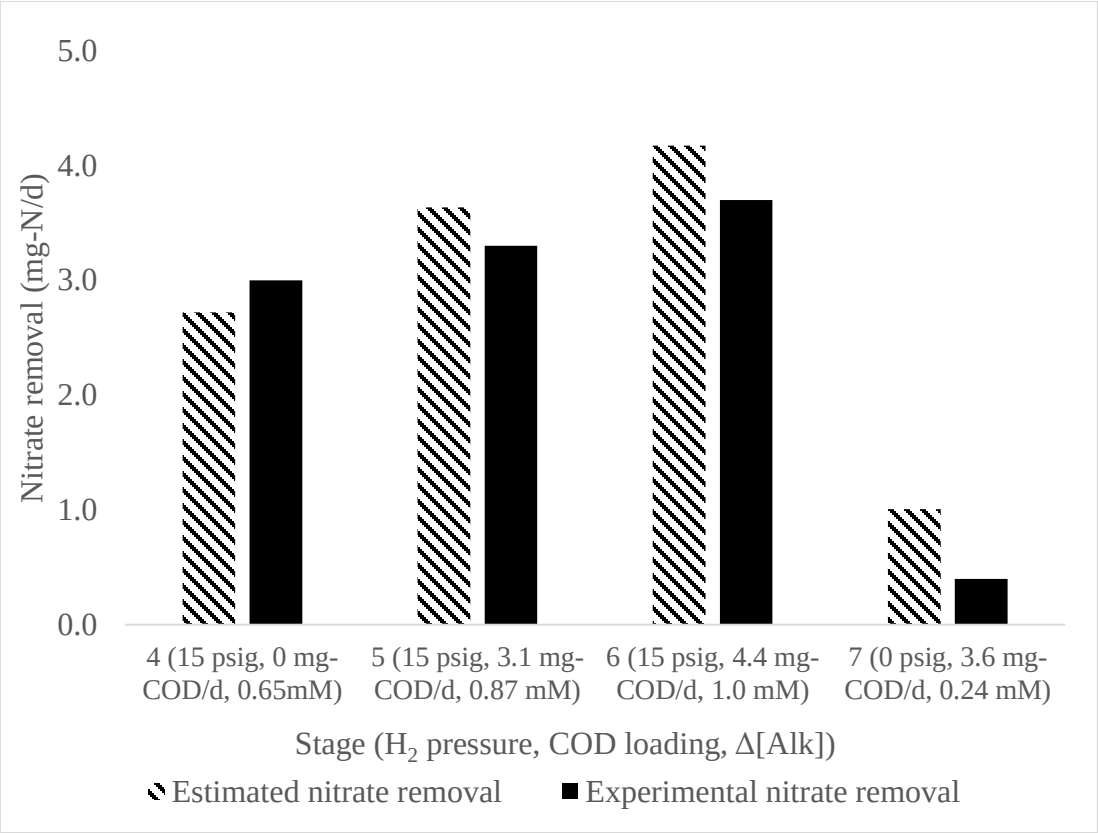

Figure 13. Comparison between the experimental mass/time nitrate removal and the mass/time nitrate removal estimate through the alkalinity change.

4.3 Conclusion

In this chapter, I derived the mathematical relationships among H_2, COD, nitrate, oxygen, and alkalinity and estimated the nitrate removal capacity for each stage. The nitrate removal based on H_2 delivery capacity and COD supply corresponded well to the experimental removal, except for stage 3, when the experimental removal was less than what could have been achieved from the H_2-delivery capacity. The most likely reason for the lower observed reduction of NO_3^- is inadequate accumulation of denitrifying bacteria

is stage 3, a topic that I explore in the next chapter. Relationships between alkalinity and nitrate provided an alternative method for the evaluating NO_3^- reduction, and the NO_3^- removal results estimated from changes in alkalinity also were consistent with experimental measurements.

CHAPTER 5

ABUNDANCE OF MICROBIAL POPULATIONS

5.1 Microbial Population Abundances in "MBfR Zone"

Figure 14 summarizes the qPCR results in cell/cm^2 for the "MBfR zone," along with the corresponding mass/time nitrate removal (in mg-N/d) for stages 2, 3, and 6. According to Figure 14, the abundance of Denitrifying Bacteria (DB) was very close to the abundance of general bacteria, which indicated that DB dominated the "MBfR zone." This trend is logical, since nitrate was the major electron acceptor for the denitrifying bacteria due to the low influent DO concentration (less than 3.5 mg/L) and lack of sulfate reduction.

An important trend from Figure 12 is that the abundance of DB was positively correlated to nitrate removal. For example, the abundance of DB for stage 3 was slightly lower than the abundance for stage 2, even though the H_2 pressure was higher in stage 3. In fact, stage 3 (with the highest H_2 pressure, Table 1) had the lowest DB abundance, as well as the mass/time nitrate removal (Table 4). A possible reason for the low DB abundance in stage 3 is the detachment of biofilm caused by the biofilm sampling at the end of stage 2. In addition, stage 3 had the lowest nitrate loading throughout the experiment, and the low nitrate loading may inhibit the growth of DB and lead to the low DB abundance in this stage. The increased H_2-supply capacity could not compensate for the lower DB abundance, and the DB did not demand all the H_2 that could have been supplied from the membranes. Thus, the input nitrate was not completely reduced, leading to the lowest experimental mass/time nitrate removal. Hence, Figure 14 helps

explain why the observed nitrate removal for stage 3 (Chapter 4) was less than the amount of nitrate removal based on the H_2-delivery capacity.

The DB abundance in stage 6 was slightly higher than that in stage 2, although the difference probably was not meaningful. A higher DB abundance in stage 6 would be consistent with the increase of heterotrophic denitrifiers caused by COD addition.

SRB were present in the isMBfR even without sulfate reduction due to their diverse metabolism, a finding seen by other MBfR researchers (Ontiveros et al., 2014; Ontiveros et al., 2012). In this case, oxygen respiration (Dilling & Cypionka, 1990) and fermentation (Muyzer & Stams, 2008) were the most likely metabolic mechanisms for the SRB. Although SRB were present, their abundance was about 1 order of magnitude lower than DB. For the same reason as for DB, stage 3 had the lowest abundance of SRB. With COD supply, stage 6 had the highest SRB abundance, because SRB can not only utilize the organics for oxygen respiration (Dannenberg et al., 1992), but also ferment lactate to acetate (Bryant et al., 1977).

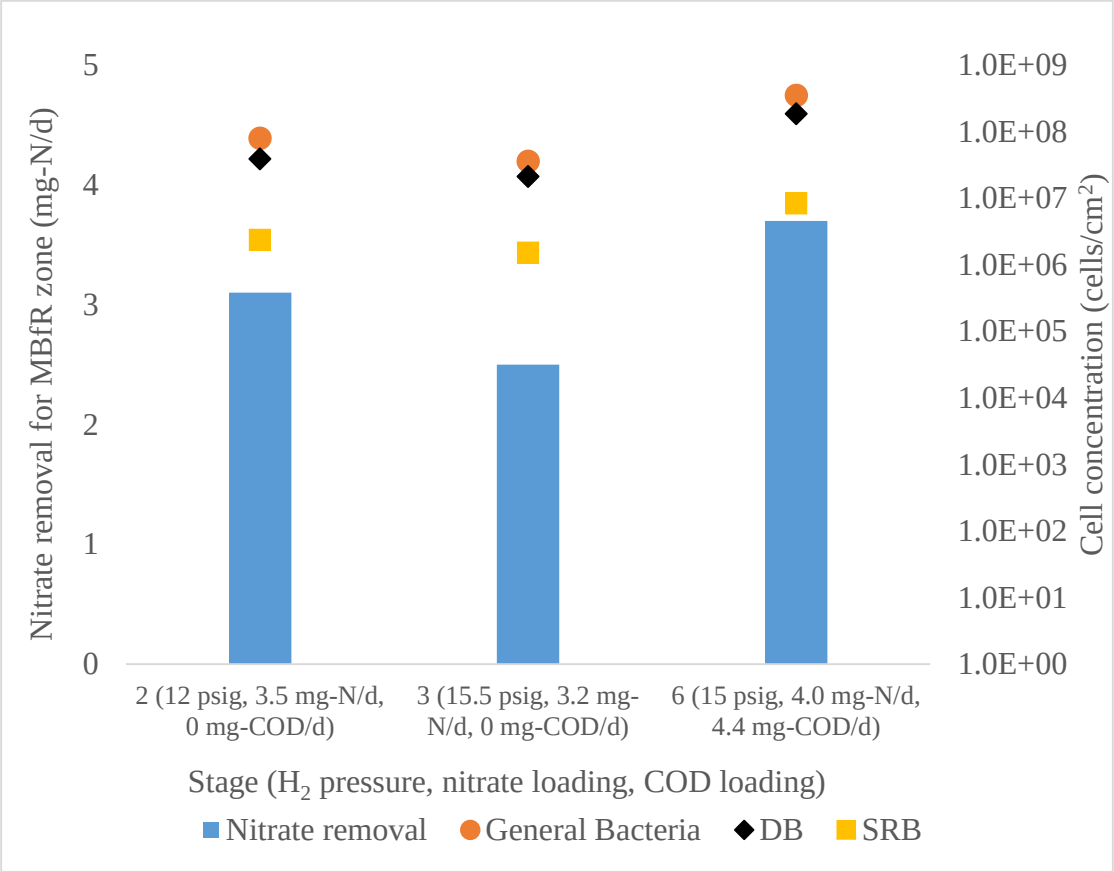

Figure 14. Abundance (in cells/cm^2) of DB, SRB, and general bacteria for stages 2, 3, and 6 in the "MBfR zone", along with nitrate removal (in mg-N/d). The H_2 pressure for these 3 stages were 12 psig, 15.5 psig, and 15 psig, respectively. The flow rates were 0.26 L/d, 0.26 L/d and 0.3 L/d, respectively. The normalization method for the bacteria cell was described in Chapter 2.

5.2 Microbial Community in "Photo-Zone"

Figure 15 summarizes the qPCR results for "photo-zone" for stages 2, 3, and 6. For stages 3 and 6, the abundance of DB in the "photo-zone" was about 3 orders of magnitude lower than in "MBfR zone" (Figure 13), which agrees with the trivial nitrate removal in this compartment (Table 4). The reason for the low DB abundance in "photo-zone" was the lack of electron donor. For all 3 stages, exogenous electron donors (H_2 and COD) were nearly completely consumed in "MBfR zone," thus "starving" DB in

"photo-zone." In addition, DB in "photo-zone," unlike "MBfR zone," had about 1 order of magnitude fewer general bacteria (Figure 15) (not 3 orders lower), indicating that DB were not the dominant bacteria in this compartment.

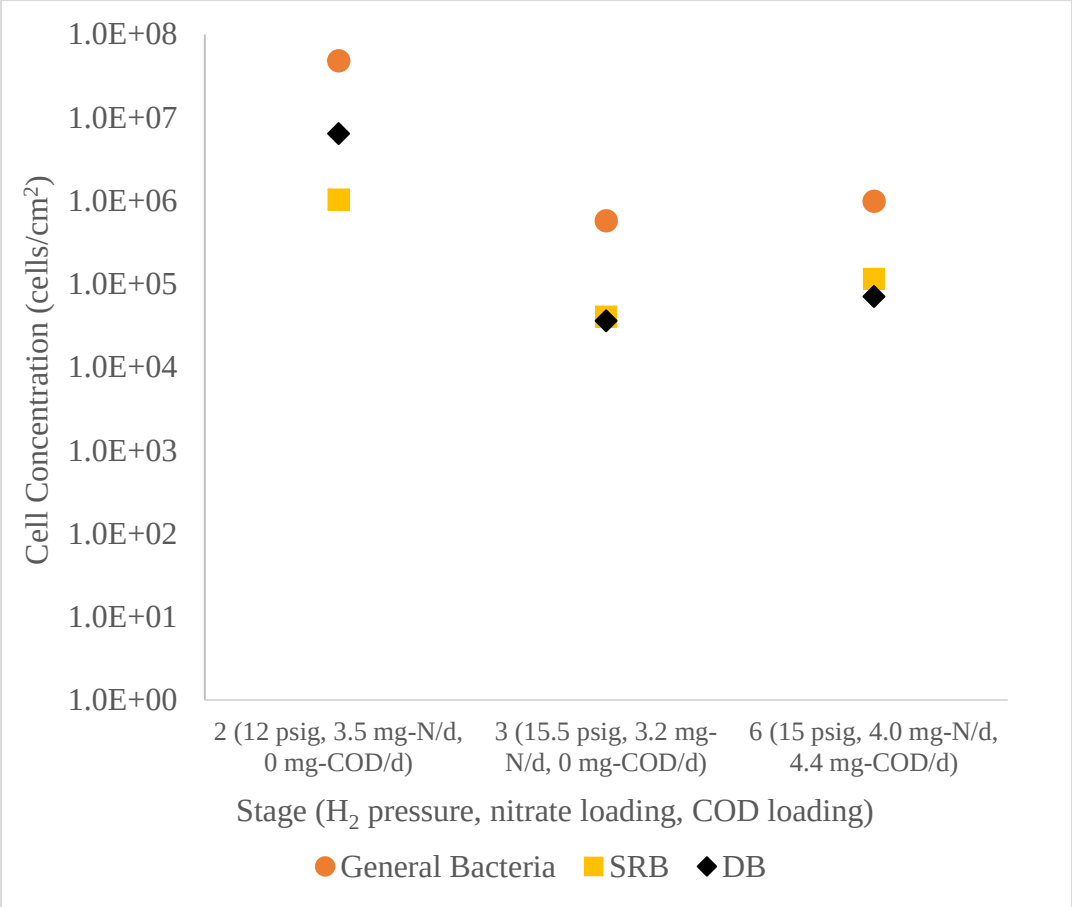

Figure 15. Abundance (in cells/cm^2) of DB, SRB, and general bacteria for stages 2, 3, and 6 in the "photo-zone." Nitrate removals were nearly 0 mg-N/d for these 3 stages. The normalization method for the bacteria cell was described in Chapter 2.

At the end of stage 6, a microbial sample was observed by light microscopy. Figures 16 and 17 show filamentous microorganisms characterized by blue-green, flexible filaments, called trichomes, that were not constricted at the cross walls. The

filaments (trichomes) were formed by cells ~ 1.8 μm in length and ~ 1.2 μm in width, and the apical cells, cells located at the tip of the filaments, were rounded. According to the characterization of filamentous cyanobacteria by Silva and Pienaar (2000), I conclude that cyanobacteria were the dominant photosynthetic microorganisms in the "photo-zone."

Figure 18 shows a pyriform shaped cell (68 μm long) with a stalk-like posterior region. According to Foissner and Berger (1996), Figure 18 shows a stalked protozoan in the "photo-zone." Since protozoa eat bacteria, an increase of protozoa may be a reason for the decrease of cell abundance from stage 2 to stage 3 (Figure 15).

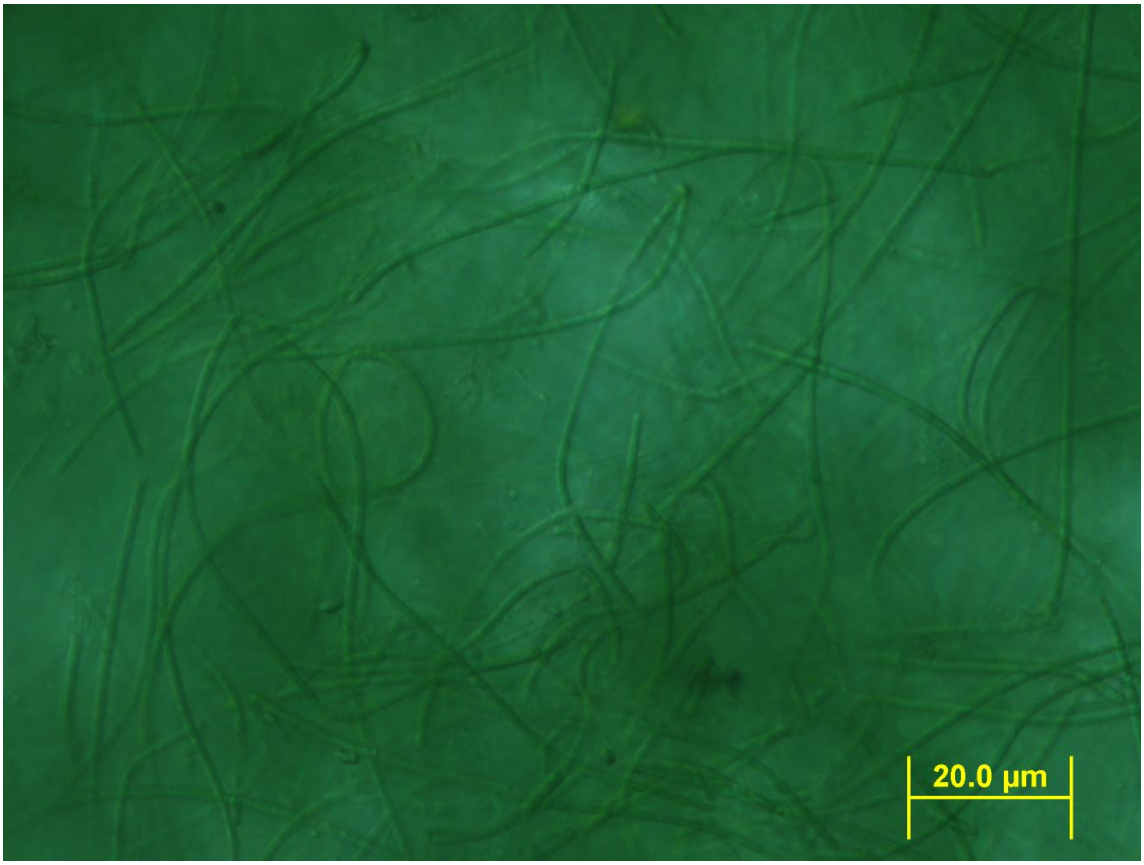

Figure 16. Cyanobacteria observed through light microscope.

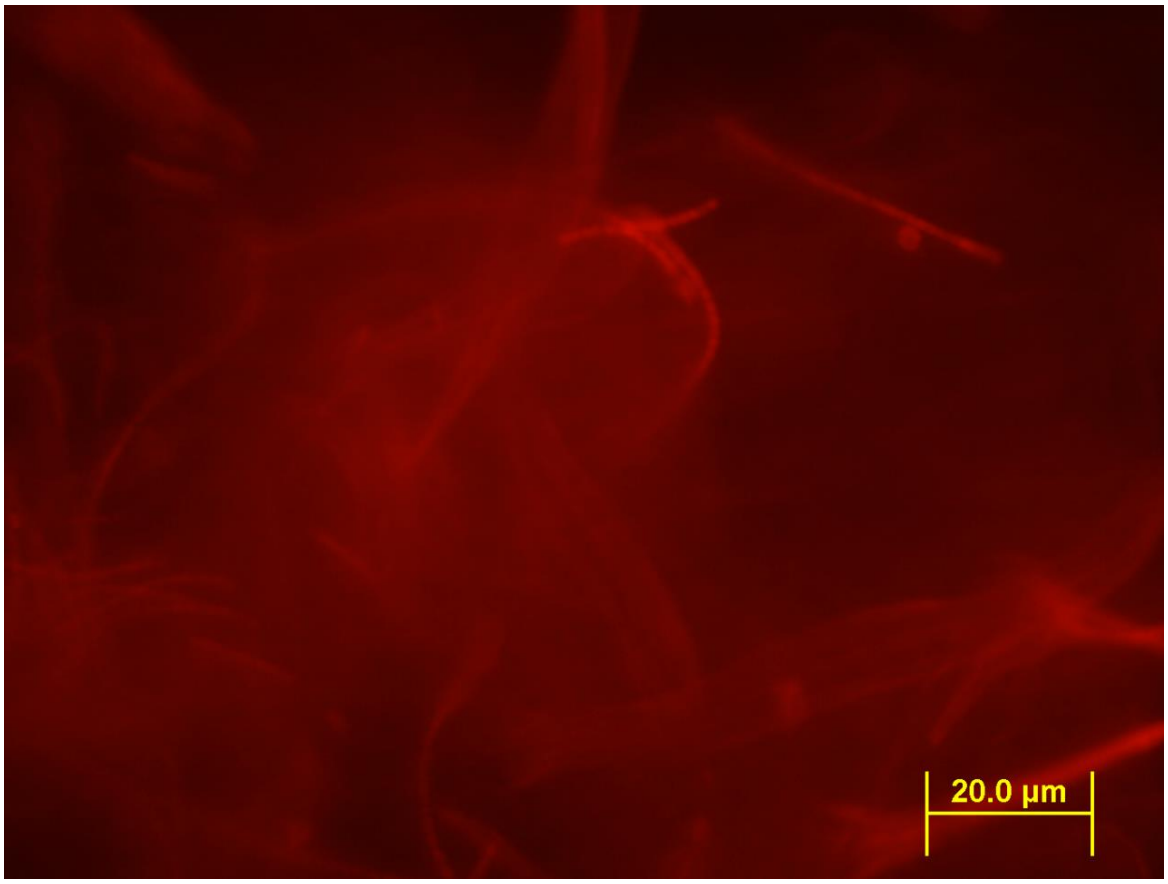

Figure 17. Fluorescent imaging of cyanobacteria.

Figure 18. A typical stalked protozoan observed through light microscope.

5.3 Conclusion

For the "MBfR zone," the high abundance of DB corresponded to the dominant nitrate respiration in the 3 stages evaluated. The relatively low abundance of DB in stage 3 can be correlated to the relatively low nitrate removal in this stage, and both can be related to the loss of biofilm during the sampling at the end of stage 2. SRB were present in "MBfR zone," but their abundance was at least 1 order of magnitude lower than DB. For the "photo-zone," DB were about 3 orders of magnitude lower than that for DB in the "MBfR zone" in stages 3 and 6, and this was due to the lack of electron donor. Finally, cyanobacteria were the dominant photosynthetic microorganisms in "photo-zone," but protozoa also were present and may have lowered the population of bacteria via grazing.

CHAPTER 6

SUMMARY, APPLICATIONS, AND RECOMMENDATIONS

6.1 Summary

The lack of exogenous electron donors usually limits the nitrate-removal capacity for a constructed wetland. The H_2-based MBfR is a means to augment the performance of constructed wetland by overcoming this inherent deficiency of constructed wetlands. The combination of an MBfR and a constructed wetland is called the *in situ* MBfR (isMBfR). With the isMBfR, H_2 is the exogenous electron donor to drive denitrification, and the nitrate-removal capacity can easily be controlled by adjusting H_2 pressure and membrane surface area.

To evaluate the potential of the isMBfR, I conducted a series of bench-scale experiments with 7 different operating conditions. For the first 6 stages, I achieved high nitrate removal percentages (at least 70%), and nearly 100% of the denitrification happened in the "MBfR zone." This demonstrates the high potential of the isMBfR for the treatment of nitrate-contaminated surface water. In stage 7, when I shut down the H_2 supply, the nitrate removal percentage dropped immediately from 92% to 11%, which indicated that H_2 was the primary electron donor in this system. This reinforces the statement that H_2-based MBfR can augment the nitrate removal capacity for a constructed wetland.

I did not detect nitrite formation or sulfate reduction during the experimental period. High pH (~ 9.0) was observed throughout the experiment in "MBfR zone" due to the consumption of protons in denitrification, but it did not impair denitrification.

Since the "MBfR zone" was almost completely responsible for nitrate removal, I modeled the nitrate removal capacity of "MBfR zone" through the stoichiometry. I derived mathematical relationships among nitrate, O_2, H_2, COD, and alkalinity. Then, I estimated the nitrate removal capacity and compared it with the experiment nitrate removal to assess the estimated values. The results indicated that the removal corresponded to the delivery capacity of H_2 and COD, except for stage 3. The qPCR results showed that stage 3 had the lowest DB abundance among stages 2, 3, and 6, even though it had the highest H_2 pressure. With such a low DB abundance, the denitrifiers did not demand all of the H_2 that could have been supplied by the membranes. Once the isMBfR system was not limited by DB abundance, nitrate removal matched the delivery capacities of H_2 and COD.

The "photo-zone" had insignificant nitrate removal throughout the experiments, and this agrees with the low DB and SRB abundances in this compartment. Since almost all of the electron donors (COD and H_2) were consumed in the "MBfR zone," the growth of DB in "photo-zone" was suppressed. Cyanobacteria were the primary photosynthetic microorganism in "photo-zone," which also had protozoa.

In conclusion, my work supports that the isMBfR can be an effective method to treat nitrate-contaminated surface water; furthermore, the nitrate-removal capacity of an isMBfR is predictable by the H_2-delivery capacity and stoichiometry. Thus, real-world application of the isMBfR system can be optimized by selecting the optimal operation conditions (e.g., H_2 pressure and membrane area).

6.2 Practical Design of the isMBfR System

In Chapter 4, I successfully modeled the nitrate removal capacity for the isMBfR system based on the operation conditions (e.g., flow rate, H_2 pressure, and influent COD concentration). In this section, I applied the modeling tool to design isMBfR systems for real wetlands to augment their nitrate-removal capacities. The goal of this section was to design a feasible operation condition (membrane area and H_2 pressure) for the real-world isMBfR application.

Before doing the designs, I made 4 assumptions: 1) the H_2 supplied to the system and the organics in the influent are entirely utilized for oxygen respiration and denitrification; 2) the amount of oxygen produced by photosynthesis or transferred from atmosphere is negligible in the "MBfR zone"; 3) denitrification contributed by electron donor generate in the wetlands is negligible; and 4) the studied wetlands are completely mixed. The treatment goal for nitrate is 0.5 mg-N/L, a level that will not cause harmful algae blooms (Biggs, 2000).

6.2.1 Case Study I: San Joaquin River National Wildlife Refuge (SJRNWR), Stanislaus County, CA

San Joaquin River National Wildlife Refuge (SJRNWR) has suffered from a high nitrate loading for a long time due to the agricultural activities in the San Joaquin Basin. Although it is restored to a managed riparian wetland by the US Fish and Wildlife Service, its nitrate-removal capacity is limited by the wetland's small size (Karpuzcu & Stringfellow, 2012). In this section, I applied the isMBfR system to the SJRNWR to augment its nitrate-removal capacity, and I designed a feasible scenario of H_2 pressure

and membrane area for this site. The characteristics for the SJRNWR are summarized in Table 10.

Table 10. Characteristics for the SJRNWR

Site	Surface area (m^2)	Flow rate (m^3/d)	Hydraulic retention time (d)	Nitrate loading (g-N/d)	COD loading (g/d)	O_2 loading (g/d)	Nitrate removal goal (g-N/d)
SJRNWR	270000	54000	5.1	380000	220000	460000	350000

Source: (Karpuzcu & Stringfellow, 2012)

Since the O_2 loading is higher than the COD loading and O_2 will be consumed first by organics oxidation, COD is considered completely removed by O_2. Again, I assume the range of f_s for autotrophic denitrification is 0 - 0.25; then, the nitrate-removal capacity for this case can be calculated by Eq. 32-33:

f_s is 0 (no biomass formation):

$$R_N = \frac{(0.0145PA_M - 0.125 \times (L_{O_2} - L_{COD}))}{0.357} \quad Eq.(32)$$

f_s is 0.25 (max biomass formation):

$$R_N = \frac{(0.0145PA_M - 0.125 \times (L_{O_2} - L_{COD}))}{0.45} \quad Eq.(33)$$

R_N is the nitrate removal capacity for the isMBfR system (g-N/d), L_{O_2} is the O_2 loading (g/d), and L_{COD} is the COD loading (g/d). When f_s = 0, all the supplied H_2 is utilized for denitrification and oxygen respiration, not biomass synthesis. This gives the minimum H_2-delivery rate and membrane area to achieve the treatment goal. The maximum

required H_2 delivery rate and membrane area occur with $f_s = 0.25$. To minimize the membrane area without incurring a risk of membrane failure, I set the H_2 pressure to 30 psig.

By substituting the nitrate capacity with the nitrate-removal goal ($R_{G,N}$, in g-N/d), I estimate the membrane area through Eq. 34 and 35:

f_s is 0 (min membrane area):

$$A_M = \frac{(0.357R_{G,N} + 0.125 \times (L_{O_2} - L_{COD}))}{0.0145P} \quad Eq.(34)$$

f_s is 0.25 (max membrane area):

$$A_M = \frac{(0.357R_{G,N} + 0.125 \times (L_{O_2} - L_{COD}))}{0.0145P} \quad Eq.(35)$$

The required membrane areas for this case are summarized in Table 11. They range from 5250 to 6350 m^2 for the flow rate of 54,000 m^3/day. In round numbers, the area requirement for this application is around 0.1 m^2 per (m^3/day). If an isMBfR module has a volume of 1 m^3 and membrane area of 300 m^2, this site of about 270,000 m^3 volume and 270,000 m^2 plan-view surface area (Table 10) would require 18 - 21 modules. The volume-specific surface area would be ~0.022 m^2 of isMBfR area per m^3 of wetland volume. This is a very modest amount of surface area, which supports the feasibility of using an isMBfR.

Table 11. A feasible scenario of H_2 pressure and membrane area for the isMBfR in SJRNWR.

	f_s	H_2 pressure (psig)	Membrane area (m^2)
min	0	30	5250
max	0.25	30	6350

6.2.2 Case Study II: 8 Wetlands of the Genevadsån Catchment, Southern Sweden

In this Swedish study area, 40 wetlands were created to remove the high nitrate loading caused by the agricultural activities. However, given the insufficient size of the wetlands, only 6% of the input nitrate can be removed (Arheimer & Wittgren, 2002), and an isMBfR seems perfectly suited. I selected 8 wetlands in the study area because they were well documented by Arheimer and Wittgren (2002). I designed a feasible isMBfR operation condition (membrane area and H_2 pressure) for each wetland. The characteristics of the 8 wetlands are summarized in Table 12.

Table 12. The characteristics of the 8 studied wetlands

Wetland	Surface area (m^2)	Flow rate (m^3/d)	Hydraulic retention time (d)	Nitrate loading (g-N/d)	COD loading (g/d)	O_2 loading[a] (g/d)	Nitrate removal goal (g-N/d)
Böslid	4000	4000	1.1	34000	0	32000	324000
Möllegård	10000	24000	0.6	130000	0	190000	120000
L. Tjärby	1000	1800	0.8	25000	0	13000	24000
S. Tjärby	3000	1400	5.0	24000	0	11000	23000
Råbytrop	8000	2400	2.5	20000	0	19000	19000
Karpalund	30000	7700	3.9	35000	0	62000	32000
Fastmårup	4000	27000	0.1	210000	0	220000	120000
Ormastorp S	5000	1900	3.6	14000	0	15000	13000

a: The influent oxygen concentration was not measured in the article; so, I used a saturated value, 8.0 mg/L, for the calculation.

Source: (Arheimer & Wittgren, 2002)

Again, I assume that the H_2 pressure is 30 psig to minimize the membrane area without inducing risk. Since organic material is not present in the influent, I can calculate the required membrane area through Eqs. 34 and 35, and the required membrane area are summarized in Table 13. In round numbers, the area requirements for

the 8 wetlands also are around 0.1 m^2 per (m^3/day). If an isMBfR module has a volume of 1 m^3 and membrane area of 300 m^2, the 8 wetlands in South Sweden (Table 12) require 2, 10, 1, 1, 1, 3, 11, and 1 modules, respectively. The volume-specific surface area would be around 0.11 m^2, 0.20 m^2, 0.15 m^2, 0.02 m^2, 0.05 m^2, 0.03 m^2, 1.2 m^2, and 0.03 m^2 of isMBfR area per m^3 of wetland volume, respectively, for the 8 wetlands. These also are very modest amount of surface area, which supports the feasibility of using an isMBfR.

Table 13. A feasible scenario of H_2 pressure and membrane area for the isMBfR in the Swedish catchment

Wetland	f_s		H_2 pressure (psig)	Membrane area (m^2)	
	min	max		min	max
Böslid	0	0.25	30	440	520
Möllegård	0	0.25	30	2700	3100
L. Tjärby	0	0.25	30	190	220
S. Tjärby	0	0.25	30	160	190
Råbytrop	0	0.25	30	270	320
Karpalund	0	0.25	30	860	1000
Fastmårup	0	0.25	30	3000	3600
Ormastorp S	0	0.25	30	210	250

6.3 Recommendations for Future Study

6.3.1 Pilot-Scale Study

My bench-scale experiments provide a good proof-of-concept of the isMBfR. However, the small size of the bench system and the lack of plant-based photo zone limit the practical applicability of my results. To provide a more realistic test of the isMBfR, a

pilot-scale study of the isMBfR should be carried out in a constructed wetland or similar setting.

When designing a pilot test, special consideration should be given to two factors:

(1) In pilot scale, oxygen may transfer from the atmosphere to the water at a higher rate than in the bench system. Also, aquatic plants may augment oxygen transfer through their root systems (Kadlec & Knight, 2008). Thus, the impacts of oxygen mass transfer may have a greater impact on H_2 delivery and should be quantified either by direct measurements or by "back calculation" based on H_2 utilization and change in DO, NO_3-, and alkalinity. Thus, the stoichiometry methods I developed here should be especially useful.

(2) An actual wetland probably will not be completely mixed. For instance, if the wetland behaves as a plug-flow reactor, we will have and need to measure a gradient in the nitrate concentration along the flow path. Perhaps a gradient of H_2 supply will be needed to avoid excessive or deficient H_2 delivery in different locations.

6.3.2 pH Control

A proper pH is an important factor to prevent sub-optimal isMBfR performance. Although the bench-scale isMBfR achieved high nitrate removal at high pH (~9), pH adjustment may be needed in some settings. Supplying CO_2 can be an effective option (Tang et al., 2011) and is used in pilot- and commercial MBfRs for end-of-pipe treatment. CO_2 is an acidic gas with high solubility. When delivered to the aquatic system, CO_2 forms carbonic acid, which compensates for the protons consumed by

denitrification. For the isMBfR, perhaps the most efficient way to deliver CO_2 is through the membrane by mixing it with H_2. This will require careful evaluation of the ratio of CO_2 to H_2 in the gas, an important research question, particularly since the solubility of CO_2 is so much greater than the solubility of H_2. Thus, bench-scale experiments and modeling analyses are needed to obtain the optimal CO_2-to-H_2 ratio for pH control.

6.3.3 Oxygenating the Effluent

In an isMBfR system, dissolved oxygen is removed by H_2 (or COD) oxidation, and the condition in the "MBfR zone" is anoxic. DO is added to the water in the "photo zone" by photosynthesis and aeration, but the effluent DO concentration was only about 4.0 mg/L in my experiments. Since DO is critical to many aquatic organisms (e.g., fish), the DO level in the effluent is of critical importance. While O_2 addition in the "photo-zone" ought to be greater in a field-scale wetland than in my bench-scale isMBfR, future testing needs to assess the effluent DO as a priority item. If the effluent DO is too low, it will need to be oxygenated.

One way for oxygenating is to sparge air into the effluent water. This method is simple and can recover the DO concentration in a short time; however, increases the operating costs for isMBfR. Another way is to build another constructed wetland after the isMBfR and recover the DO concentration through oxygen transfer and photosynthesis. This method does not involve operation cost, but it involves land usage and capital costs.

REFERENCES

Arheimer, B., & Wittgren, H.B. (2002). Modelling nitrogen removal in potential wetlands at the catchment scale. *Ecological Engineering 19*, 63-80.

Beutel, M.W., Newton, C.D., Brouillard, E.S., & Watts, R.J. (2009). Nitrate removal in surface-flow constructed wetlands treating dilute agricultural runoff in the lower Yakima Basin, Washington. *Ecological Engineering, 35*, 1538-1546.

Biggs, B.J.F. (2000). Eutrophication of streams and rivers: dissolved nutrient–chlorophyll relationships for benthic algae. *J. N. Am. Benthol. Soc., 19*, 17-31.

Bryant, M.P., Campbell, L.L., Reddy, C.A., & Crabill, M.R. (1977). Growth of Desulfovibrio in lactate or ethanol media low in sulfate in association with H_2-utilizing methanogenic bacteria. *Appl. Environ. Microbiol., 33*, 1162-1169.

Camargo, J.A., Alonso, A., & Salamanca, A. (2005). Nitrate toxicity to aquatic animals: a review with new data for freshwater invertebrates. *Chemosphere, 58*, 1255-1267.

Carpenter, S.R., Bolgrien, D., Lathrop, R.C., Stowe, C.A., Reed, T., & Wilson, M.A. (1997). Ecological and economic analysis of lake eutrophication by nonpoint pollution. *Australian Journal of Ecology, 23*, 68-79.

Cheng, S.-Y., & Chen, J.-C. (2002). Study on the oxyhemocyanin, deoxyhemocyanin, oxygen affinity and acid–base balance of Marsupenaeus japonicus following exposure to combined elevated nitrite and nitrate. *Aquatic Toxicol, 61*, 181-193.

Chung, J., Krajmalnik-Brown, R., & Rittmann, B.E. (2008). Bioreduction of trichloroethene using a hydrogen-based membrane biofilm reactor. *Environ. Sci. Technol., 42*(2), 477-483.

Coates, J.D., Chakraborty, R., Lack, J.G., O'Connor, S.M., Cole, K.A., Bender, K.S., & Achenbach, L.A. (2001). Anaerobic benzene oxidation coupled to nitrate reduction in pure culture by two strains of Dechloromonas. *Nature, 411*, 1039-1043.

Collins, K.A., Lawrence, T.J., Stander, E.K., Jontos, R.J., Kaushal, S.S., Newcomer, T.A., Grimm, N.B., & Ekberg, M.L. (2010). Opportunities and challenges for managing nitrogen in urban stormwater: A review and synthesis. *Ecological Engineering, 36*, 1507-1519.

Dannenberg, S., Kroder, M., Dilling, W., & Cypionka, H. (1992). Oxidation of H_2, organic compounds and inorganic sulfur compounds coupled to reduction of O_2 or nitrate by sulfate-reducing bacteria. *Archives of Microbiology, 158*(2), 93-99.

Day, J.W., Ko, J.Y., Rybczyk, J., Sabins, D., Bean, R., Berthelot, G., Brantley, C., Cardoch, L., Conner, W., Day, J.N., Englande, A.J., Feagley, S., Hyfield, R., Lindsey, J., Mistich, J., Reyes, E., & Twilley, R. (2004). The use of wetlands in the Mississippi Delta for wastewater assimilation: a review. *Ocean Coast. Manage., 47,* 671-691.

Dilling, W., & Cypionka, H. (1990). Aerobic respiration in sulfate-reducing bacteria. *FEMS Microbiol. Lett., 71*, 123−128.

Evans, P.J., Smith, J.L., Singh, T.S., Hoon, H., Arucan, C., Berokoff, D., Friese, D., Overstreet, R., Vigo, R., Rittmann, B.E., Ontiveros-Valencia, A., Zhao, H.P., Tang, Y., Kim, B.O., Van Ginkel, S., & Krajmalnik-Brown, R. (2013). Nitrate and perchlorate destruction and potable water production using membrane biofilm reduction. ESTCP Project ER-200541

Fogel, G.B., Collins, C.R., Li, J., & Brunk, C.F. (1999). Prokaryotic genome size and ssu rDNAcopy number: estimation of microbial relative abundance from a mixed population. *Microb. Ecol., 38*, 93-113.

Foissner, W., & Berger, H. (1996). A user-friendly guide to the ciliates (protozoa, ciliophora) commonly used by hydrobiologists as bioindicators in river, lakes and wastewater, with notes. *Freshwater Biology, 35*, 375-482.

Groffman, P.M., Law, N.L., Belt, K.T., Band, L.E., & Fisher, G.T. (2004). Nitrogen fluxes and retention in urban watershed ecosystems. *Ecosystems, 7*, 393-403.

Hasar, H., Xia, S., Ahn, C.H., & Rittmann, B.E. (2008). Simultaneous removal of organic matter and nitrogen compounds by an aerobic/anoxic membrane biofilm reactor. *Water Research, 42*(15), 4109-4116.

Jensen, F.B. (1996). Uptake, elimination and effects of nitrite and nitrate in freshwater crayfish (Astacus astacus). *Aquatic Toxicol, 34*, 95-104.

Kadlec, R.H., & Knight, R.L. (2008). *Treatment wetlands, Second Edition*: CRC Press.

Karpuzcu, M.E., & Stringfellow, W.T. (2012). Kinetics of nitrate removal in wetlands receiving agricultural drainage. *Ecological Engineering, 42*, 295-303.

Kondo, R., Nedwell, D.B., Purdy, K.J., & Quiroz Silva, S. (2004). Detection and enumeration of sulphate-reducing bacteria in estuarine sediments by competitive PCR. *J. Geomicrobiology, 21*, 145-157.

Laspidou, C.S., & Rittmann, B.E. (2002). A unified theory for extracellular polymeric substances, soluble microbial products, and active and inert biomass. *Water Research, 36*, 2711-2720.

Lee, K.C., & Rittmann, B.E. (2000). A novel hollow-fibre membrane biofilm reactor for autohydrogenotrophic denitrification of drinking water. *Water Sci. Technol., 41*, 219-226.

Lee, K.C., & Rittmann, B.E. (2002). Applying a novel autohydrogenotrophic hollow-fiber membrane biofilm reactor for denitrification of drinking water. *Water Research, 36*, 2040-2052.

Lee, K.C., & Rittmann, B.E. (2003). Effects of pH and precipitation on autohydrogenotrophic denitrification using the hollow-fiber membrane-biofilm reactor. *Water Research, 37*, 1551-1556.

Lynch, J.M. (1990). Introduction: some consequences of microbial rhizosphere competence for plant and soil. In J. M. Lynch (Ed.), *The rhizosphere* (pp. 1-10). Chichester: John Wiley.

Mansor, M., Lim, P.E., & Shutes, R.B.E. (2002). *Constructed wetlands : design, management and education*. Pulau Pinang, Malaysia: Penerbit Universiti Sains Malaysia.

Martin, K.J., & Nerenberg, R. (2012). The membrane biofilm reactor (MBfR) for water and wastewater treatment: principles, applications, and recent developments. *Bioresource Technology, 122*, 83-94.

McGechan, M.B., Moir, S.E., Sym, G., & Castle, K. (2005). Estimating inorganic and organic nitrogen transformation rates in a model of a constructed wetland purification system for dilute farm effluents. *Biosyst. Eng., 91*, 61-75.

Muyzer, G., & Stams, A.J.M. (2008). The ecology and biotechnology of sulphate-reducing bacteria. *Nat. Rev. Microbiol., 6*, 441−454.

Ontiveros, A., Tang, Y., Krajmalnik-Brown, R., & Rittmann, B.E. (2014). Managing the interactions between sulfate- and perchlorate-reducing bacteria when using hydrogen-fed biofilms to treat a groundwater with a high perchlorate concentration. *Water Research, 55*, 215-224.

Ontiveros, A., Ziv-El, M.C., Zhao, H., Feng, L., Rittmann, B.E., & Krajmalnik-Brown, R. (2012). Interactions between nitrate-reducing and sulfate-reducing bacteria coexisting in a hydrogen-fed biofilm. *Environ. Sci. Technol., 40*(20), 11289–11298.

Philippot, L. (2006). Use of functional genes to quantify denitrifiers in the environment. *Biochem. Soc. Trans., 34*, 101-103.

Poe, A.C., Piehler, M.F., Thompson, S.P., & Paerl, H.W. (2003). Denitrification in a constructed wetland receiving agricultural runoff. *The Society of Wetland Scientists, 23*(4), 817-826.

Rittmann, B.E. (2013). *US Patent No. 8,394,273.*

Rittmann, B.E., & McCarty, P.L. (2001). *Environmental Biotechnology: Principles and Application*. New York: McGraw-Hil Book Co.

Silva, D.G., & Rittmann, B.E. (2000). Interpreting the response to loading changes in a mixed-culture completely stirred tank reactor. *Water Environment Research, 72*, 566-573.

Silva, M.F., & Pienaar, R.N. (2000). *Bethic Marine Cyanophyceae from Kwa-Zulu Natal, South Africa*. Berlin: Gebrüder Borntraeger Verlagsbuchhandlung.

Smith, V.H., Tilman, G.D., & Nekola, J.C. (1999). Eutrophication: impacts of excess nutrient inputs on freshwater, marine, and terrestrial ecosystems. *Environmental Pollution, 100*, 179-196.

Stevenson, D.G. (1997). *Waste treatment unit processes*. London: Imperial College Press.

Tang, Y., Scott, R., Rittmann, B.E., Ziv-El, M.C., Zhou, C., Shin, J.H., & Overstreet, R. (2010). Bioreduction of nitrate in groundwater using a pilot-scale hydrogen-based membrane biofilm reactor. *Frontiers of Environmental Science & Engineering in China, 4*, 280-285.

Tang, Y., Zhou, C., Van Ginkel, S.W., Ontiveros, A., Shin, J., & Rittmann, B.E. (2012). Hydrogen permeability of the hollow fibers used in H_2-based membrane biofilm reactor. *Journal of Membrane Science, 407-408*, 176-183.

Tang, Y., Zhou, C., Ziv-El, M.C., & Rittmann, B.E. (2011). A pH-control model for heterotrophic and hydrogen-based autotrophic denitrification. *Water Research, 45*, 232-240.

US Environmental Protection Agency. (1986). *Quality criteria for water*. (EPA 440/5-86-001). Washington, DC.

Vagnetti, R., Miana, P., Fabris, M., & Pavoni, B. (2003). Self-purification ability of a resurgence stream. *Chemosphere, 52*(10), 1781-1795.

Van Ginkel, S.W, Yang, Z., Kim, B.O., Sholin, M., & Rittmann, B.E. (2011). The removal of selenate to low ppb levels from flue gas desulfurization brine using the H_2-based membrane biofilm reactor (MBfR). *Bioresource Technology, 102*, 6360-6364.

Vitousek, P.M., & Howarth, R.W. (1991). Nitrogen limitation on land and in the sea - how can it occur. *Biochemestry, 13*, 87-115.

WHO. (2004). *Rolling revision of the WHO guidelines for drinking-water quality: nitrates and nitrites in drinking-water*. Retrieved from http://www.who.int/water_sanitation_health/dwq/chemicals/en/nitratesfull.pdf.

Zhao, H., Ontiveros, A., Tang, Y., Kim, B.O., Van Ginkel, S.W., Friese, D., & Rittmann, B.E. (2014). Removal of multiple electron acceptors by pilot-scale, two-stage membrane biofilm reactors. *Water Research, 54*, 115-122.

Ziv-El, M.C., & Rittmann, B.E. (2009). Systematic evaluation of nitrate and perchlorate bioreduction kinetics in groundwater using a hydrogen-based membrane biofilm reactor. *Water Research, 43*, 173-181.